Discovery of biased orientations of human regulatory motifs affecting transcription of genes and including known insulators

Naoki Osato[1*]

[1]Department of Bioinformatic Engineering, Graduate School of Information Science and Technology, Osaka University, Osaka 565-0871, Japan

[*]Corresponding author

E-mail address: naokiosato11@gmail.com, nosato@ist.osaka-u.ac.jp

Abstract

Chromatin interactions have important roles for enhancer-promoter interactions (EPIs) and regulating the transcription of genes. CTCF and cohesin proteins are located at the anchors of chromatin interactions, forming their loop structures. CTCF has insulator function limiting the activity of enhancers into the loops. DNA binding sequences of CTCF indicate their orientation bias at chromatin interaction anchors – forward-reverse (FR) orientation is frequently observed. Other DNA binding proteins such as YY1, ZNF143 and SMARCA4 are also reported to be associated with chromatin interactions. It is still unclear what proteins are associated with chromatin interactions and insulator function.

To find DNA binding motif sequences of transcription factors (TFs) like CTCF, affecting the interaction between enhancers and promoters of genes and their expression by the insulator function of the TFs, first, I predicted TF bound in enhancers and promoters using DNA motif sequences of TFs and experimental data of open chromatin regions in monocytes, T, Th17, Treg, GM12878 cells, HMEC and NPC, which were obtained from public and commercial databases. Second, transcriptional target genes of each TF were predicted based on enhancer-promoter association (EPA). An EPA was shortened at the FR or reverse-forward (RF) orientation of DNA motif sites of a TF, which were supposed to be at chromatin interaction anchors and acted as insulator sites. Then, the expression levels of transcriptional target genes predicted based on the EPA were compared with those predicted from closed chromatin regions.

Total 96 biased orientations of DNA motifs (64 FR and 52 RF orientations, the

reverse complement sequences of some DNA motifs were also registered in databases, so the total number was smaller than the number of FR and RF) affected the expression level of putative transcriptional target genes significantly in monocytes, T cells, HMEC and NPC in common, including known TFs associated with chromatin interaction and insulator function such as CTCF, cohesin (RAD21 and SMC3), YY1 and ZNF143. Compared with chromatin interaction data, for 44 (69%) FR and 28 (54%) RF orientations of DNA motif sequences in $CD4^+$ T cells, EPIs predicted from EPAs that were shortened at the biased orientations of DNA motif sites, overlapped with chromatin interactions significantly more than other types of EPAs. Using gene expression data among 53 tissues, 43 (72%) FR and 40 (80%) RF orientations of DNA motifs showed significantly reduced correlation in expression level of nearby genes separated by the motif sites. These analyses suggest that the DNA motifs are associated with insulator functions.

Keywords: transcriptional target genes, gene expression, transcription factors, enhancer, enhancer-promoter interactions, chromatin interactions, CTCF, cohesin, open chromatin regions, co-location of transcription factors, homodimer, heterodimer, complex

Background

Chromatin interactions have important roles for enhancer-promoter interactions (EPIs) and regulating the transcription of genes. CTCF and cohesin proteins are located at the anchors of chromatin interactions, forming their loop structures. CTCF has

55 insulator function limiting the activity of enhancers into the loops (Fig. 1A). The DNA
56 binding sequence of CTCF indicate its orientation bias at chromatin interaction anchors
57 – forward-reverse (FR) orientation is frequently observed (Rao et al. 2014; de Wit et al.
58 2015; Guo et al. 2015). Other DNA binding proteins such as ZNF143, YY1 and
59 SMARCA4 (BRG1) are found to be associated with chromatin interaction and EPI
60 (Bailey et al. 2015; Barutcu et al. 2016; Weintraub et al. 2017). CTCF, cohesin, ZNF143,
61 YY1 and SMARCA4 have other biological functions as well as chromatin interaction
62 and EPI. The DNA binding motif sequences of these transcription factors (TFs) are
63 found in open chromatin regions near transcriptional start sites (TSS) as well as
64 chromatin interaction anchors.

65 DNA binding motif sequence of ZNF143 was enriched at both chromatin
66 interaction anchors. ZNF143's correlation with the CTCF-cohesin cluster relies on its
67 weakest binding sites, found primarily at distal regulatory elements defined by the
68 'CTCF-rich' chromatin state. The strongest ZNF143-binding sites map to promoters
69 bound by RNA polymerase II (POL2) and other promoter-associated factors, such as the
70 TATA-binding protein (TBP) and the TBP-associated protein, together forming a
71 'promoter' cluster (Bailey et al. 2015).

72 DNA binding motif sequence of YY1 does not seem to be enriched at both
73 chromatin interaction anchors (Z-score < 2), whereas DNA binding motif sequence of
74 ZNF143 is significantly enriched (Z-score > 7; Bailey et al. 2015 Figure 2a). In the
75 analysis of YY1, to identify a protein factor that might contribute to EPI, (Ji et al. 2015)
76 performed chromatin immune precipitation with mass spectrometry (ChIP-MS), using

77 antibodies directed toward histones with modifications characteristic of enhancer and
78 promoter chromatin (H3K27ac and H3K4me3, respectively). Of 26 transcription factors
79 that occupy both enhancers and promoters, four are essential based on a CRISPR
80 cell-essentiality screen and two (CTCF, YY1) are expressed in >90% of tissues
81 examined (Weintraub et al. 2017). This research started from the analysis of histone
82 modifications of enhancer and promoter marks rather than chromatin interactions. Other
83 protein factors associated with chromatin interaction and insulator function may be
84 found from other researches.

85 As computational approaches, machine-learning analyses to predict chromatin
86 interactions were proposed (Schreiber et al. 2017; Zhang et al. 2017). However, they
87 were not intended to find DNA motif sequences of TFs affecting chromatin interaction,
88 EPI and the expression level of transcriptional target genes, which were examined in
89 this study.

90 DNA binding proteins involved in chromatin interactions are supposed to affect
91 the transcription of genes in the loops formed by chromatin interactions. To analyze this
92 property, I found that the expression level of human putative transcriptional target genes
93 of a TF was significantly changed, according to the criteria of enhancer-promoter
94 association (EPA) (Osato 2018). An EPA was shortened at the FR orientation of CTCF
95 binding sites, and transcriptional target genes of each TF bound in enhancers and
96 promoters were predicted based on the EPA (Fig. 1B). The expression levels of
97 transcriptional target genes were significantly changed, compared with the expression
98 levels of transcriptional target genes predicted from promoters (or closed chromatin

99 regions). The expression levels tend to be increased in monocytes and $CD4^+$ T cells,
100 implying that enhancers activate the transcription of genes. The expression levels tend
101 to be decreased in ES and iPS cells, implying that enhancers repress the transcription of
102 genes. These analyses showed that the expression level of putative transcriptional target
103 genes of a TF bound in enhancers was changed significantly, as EPIs were predicted
104 properly using insulator sites of CTCF. This suggests that the difference of the
105 expression level would be an index of the accuracy of the prediction of transcriptional
106 target genes of a TF based on an EPA. Other DNA binding proteins involved in
107 chromatin interactions as well as CTCF may locate at chromatin interaction anchors
108 with a pair of biased orientation of DNA binding motif sites, affecting the expression
109 level of putative transcriptional target genes through their insulator function.

110 As experimental issues of analyses of chromatin interactions, chromatin
111 interaction data are changed, according to experimental techniques, the number of reads
112 of DNA sequencing and even replication sets of the same cell type. Chromatin
113 interaction data may not be saturated enough to contain all chromatin interactions and
114 may include experimental noise such as ligation error. Supposing the properties of DNA
115 binding proteins associated with chromatin interactions and avoiding experimental
116 issues of analyses of chromatin interactions, here I searched for DNA motif sequences
117 of TFs, affecting EPI and the expression level of putative transcriptional target genes in
118 monocytes, T cells, HMEC and NPC without using chromatin interaction data. Then,
119 putative EPIs were compared with chromatin interaction and gene expression data.
120

Results

Search for biased orientations of DNA motif sequences

Transcription factor binding sites (TFBSs) were predicted using open chromatin regions and DNA motif sequences of transcription factors (TF) collected from various databases and journal papers (see Methods). Transcriptional target genes were predicted using TFBS in promoters and enhancers. An enhancer-promoter association (EPA) was shortened at the DNA binding motif sites of a TF acting as insulator such as CTCF and cohesin (RAD21 and SMC3) (Fig. 1B). To find DNA motif sequences of TF acting as insulator, other than CTCF and cohesin, affecting the expression level of genes, An EPA was shortened at the DNA motif sites of a putative insulator TF, and transcriptional target genes of each general TF bound in (i) distal open chromatin regions (enhancers) and (ii) closed chromatin regions in promoters were predicted based on the EPA, in order to estimate enhancer activity of each TF. The ratio of expression level of putative transcriptional target genes of each TF between (i) and (ii) was calculated. The distribution of the ratios of all TF was compared among forward-reverse (FR), reverse-forward (RF) and any orientation (i.e. without considering orientation) of DNA motif sites of an insulator TF shortening EPA using Mann-Whitney test, two-sided (p-value < 10^{-7}), and the number of putative insulator TFs with significant difference of the distributions of expression level among FR, RF and Any was counted (Fig. 2A). To check the prediction of DNA motif sites of TFs, the distribution of DNA motif sites were examined in the human genome. DNA motif sites of TFs associated with chromatin interactions were found near TSS (Fig. 2B). ZNF143 is known to bind to

143 promoter of genes establishing looping with distal element bound by CTCF (Fig. 5)
144 (Bailey et al. 2015). YY1 is multi-functional transcriptional regulator and is involved in
145 transcriptional activation, repression and initiation (Shrivastava and Calame 1994; Xi et
146 al. 2007). Most of DNA sites of the TFs were found in intergenic and intron regions of
147 the human genome (Fig. 2C). Several hundreds of FR and RF orientations of DNA
148 motifs of TFs were found in monocytes, T cells, human mammary epithelial cells
149 (HMEC) and neural progenitor cells (NPC) (Fig. 3). The number of the TFs seemed to
150 be changed, according to the number of DNase-seq reads, since the number of the reads
151 in monocyte is larger than the other three cell types. When DNase-seq reads increase,
152 more DNA motif sites may be predicted to some extent. Total 96 of biased (64 FR and
153 52 RF) orientations of DNA binding motif sequences of TFs were found in the four cell
154 types in common, whereas any orientation of DNA binding motif sequence was not
155 found (Fig. 3; Table 1; Supplemental material). The FR orientation of DNA motif
156 sequences included CTCF, cohesin (RAD21 and SMC3), YY1 and ZNF143, which are
157 associated with chromatin interaction and EPI.

158 Without considering the difference of orientations of DNA binding motif
159 sequences among cell types, 175 of biased orientations of DNA binding motif
160 sequences of TFs were found in the four cell types in common. These numbers (96 and
161 175) are unique number of TFs with biased orientation of DNA motifs, and not the
162 number of DNA motifs. As one of reasons for the increase of the number 175 from 96, a
163 TF or an isoform of the same TF may bind to a different DNA binding motif sequence,
164 according to cell types and/or in the same cell type. About 50% or more of alternative

splicing isoforms are differently expressed among tissues, indicating that most alternative splicing is subject to tissue-specific regulation (Das et al. 2007; Wang et al. 2008; Chen and Manley 2009). As another reason, the same TF has several DNA binding motif sequences and in some cases one of the motif sequences is almost the same as the reverse complement sequence of another motif sequence of the same TF. Moreover, I previously found that a complex of TF would bind to a slightly different DNA binding motif sequence from the combination of DNA binding motif sequences of TFs composing the complex in *C. elegans* (Tabuchi et al. 2011). The difference of binding specificity of pairs of transcription factors was reported (Jolma et al. 2015). Cofactors also contribute to alter binding specificity of transcription factors (Ansari and Peterson-Kaufman 2011; Slattery et al. 2011; Merabet and Mann 2016). These increase the variety and number of (biased orientations of) DNA binding motif sequences of a TF, which are potentially involved in different biological functions among cell types.

Comparison with chromatin interaction data

To examine whether the biased orientations of DNA motif sequences are associated with chromatin interaction, enhancer-promoter interactions (EPIs) predicted based on an enhancer-promoter association (EPA) were compared with chromatin interaction data. HiChIP chromatin interaction data were used for $CD4^+$ T cells (Mumbach et al. 2017). EPIs predicted based on an EPA were compared with three replications (B2T1, B2T2 and B3T1) of HiChIP chromatin interaction data respectively. The resolutions of HiChIP chromatin interaction data and EPIs were adjusted to 5

187 kilobases (kb). EPI were predicted based on three types of EPAs: (i) EPA shortened at
188 the FR or RF orientation of DNA motif sites of a TF acting as insulator such as CTCF,
189 (ii) EPA shortened at the DNA motif sites of a TF without considering their orientation,
190 and (iii) EPA without being shortened by DNA motif sites. Total 201 biased orientations
191 [133 (49%) FR and 90 (43%) RF of 273 FR and 211 RF] of DNA motif sequences in T
192 cells, which included CTCF, cohesin (RAD21 and SMC3), ZNF143 and YY1 in three
193 replications (B2T1, B2T2, and B3T1), showed a significantly higher ratio of EPIs
194 overlapped with HiChIP chromatin interactions with ≥1,000 counts for each interaction
195 in EPA (i) than the other types of EPA (ii) and (iii) in T cells (Table 2). When comparing
196 EPIs predicted based on only EPA (i) and (iii) with the chromatin interactions, total 390
197 biased orientations [261 (96%) FR and 199 (94%) RF of 273 FR and 211 RF] of DNA
198 motif sequences in T cells showed a significantly higher ratio of EPIs overlapped with
199 the chromatin interactions in EPA (i) than EPA (iii) (Table 2; Supplemental material).
200 The difference between EPIs predicted based on EPA (i) and (ii) seemed to be difficult
201 to distinguish using the chromatin interaction data and statistical test in some cases.
202 However, as for the difference between EPIs predicted based on EPA (i) and (iii), a
203 larger number of biased orientations of DNA motif sequences were found to be
204 correlated with chromatin interaction data. Chromatin interaction data were obtained
205 from different samples from DNase-seq open chromatin regions, so individual
206 differences may exist. (Mumbach et al. 2017) suggested that individual differences of
207 chromatin interactions were larger than those of open chromatin regions. Most of biased
208 orientations of DNA motif sequences (95%) were found to be correlated with chromatin

209 interactions, when comparing EPIs predicted based on EPA (i) and (iii) with HiChIP
210 chromatin interactions.

211 Additionally, to confirm these tendencies of comparison of EPIs with HiChIP
212 chromatin interactions, the same analysis was conducted using HiChIP chromatin
213 interaction data in Th17, Treg and GM12878 cells. Total 128 biased orientations [76
214 (38%) FR and 64 (35%) RF of 200 FR and 183 RF] of DNA motif sequences in Th17
215 cells, which included CTCF, cohesin (RAD21 and SMC3), ZNF143 and YY1 in three
216 replications (B1T2, B2T1, and B3T1), showed a significantly higher ratio of EPIs
217 overlapped with HiChIP chromatin interactions in EPA (i) than the other types of EPA
218 (ii) and (iii) (Supplemental material). When comparing EPIs predicted based on only
219 EPA (i) and (iii) with the chromatin interactions, total 282 biased orientations [182
220 (91%) FR and 162 (89%) RF of 200 FR and 183 RF] of DNA motif sequences showed a
221 significantly higher ratio of EPIs overlapped with the chromatin interactions in EPA (i)
222 than EPA (iii) (Supplemental material).

223 For Treg cells, chromatin interactions in one biological replication were
224 overlapped with EPIs, but those in the other two biological replications were less
225 overlapped with EPIs, so the one replication (B3T1) was used for this analysis. Total
226 281 biased orientations [154 (53%) FR and 176 (54%) RF of 290 FR and 323 RF] of
227 DNA motif sequences, which included CTCF, cohesin (RAD21 and SMC3), ZNF143
228 and YY1, showed a significantly higher ratio of EPIs overlapped with HiChIP
229 chromatin interactions in EPA (i) than the other types of EPA (ii) and (iii) (Supplemental
230 material). When comparing EPIs predicted based on only EPA (i) and (iii) with the

chromatin interactions, total 482 biased orientations [283 (98%) FR and 309 (96%) RF of 290 FR and 323 RF] of DNA motif sequences showed a significantly higher ratio of EPIs overlapped with the chromatin interactions in EPA (i) than EPA (iii) (Supplemental material).

For GM12878 cells, total 168 biased orientations [96 (38%) FR and 98 (35%) RF of 229 FR and 237 RF] of DNA motif sequences, which included CTCF, cohesin (RAD21 and SMC3), ZNF143 and YY1 in two replications (B1 and B2), showed a significantly higher ratio of EPIs overlapped with HiChIP chromatin interactions in EPA (i) than the other types of EPA (ii) and (iii) (Supplemental material). When comparing EPIs predicted based on only EPA (i) and (iii) with the chromatin interactions, total 366 biased orientations [218 (95%) FR and 227 (96%) RF of 229 FR and 237 RF] of DNA motif sequences showed a significantly higher ratio of EPIs overlapped with the chromatin interactions in EPA (i) than EPA (iii) (Supplemental material).

In situ Hi-C data was available from 4D nucleome data portal in HMEC, and was compared with putative EPIs. Total 222 biased orientations [155 (50%) FR and 108 (40%) RF of 310 FR and 269 RF] of DNA motif sequences, which included CTCF, cohesin (RAD21 and SMC3), ZNF143 and YY1, showed a significantly higher ratio of EPIs overlapped with in situ Hi-C chromatin interactions ($\geq$1 count for each interaction, i.e. all interactions) in EPA (i) than the other types of EPA (ii) and (iii) (Supplemental material). When comparing EPIs predicted based on only EPA (i) and (iii) with the chromatin interactions, total 406 biased orientations [268 (86%) FR and 230 (86%) RF of 310 FR and 269 RF] of DNA motif sequences showed a significantly higher ratio of

253 EPIs overlapped with the chromatin interactions in EPA (i) than EPA (iii) (Supplemental
254 material). There were six replications of in situ Hi-C experimental data of HMEC, but
255 other replications contained much smaller number of chromatin interactions. The
256 HiChIP chromatin interaction data in T cells were expected to be enriched with
257 enhancer-promoter interactions, since it used H3K27ac antibody to collect chromatin
258 interactions. In situ Hi-C data contain all types of chromatin interactions and thus,
259 contain a smaller number of enhancer-promoter interactions, relative to HiChIP data.
260 Chromatin interactions with a small number of counts may be artifacts derived from
261 ligation errors during experiments (Lieberman-Aiden et al. 2009; Yardimci et al. 2019).
262 Therefore, other replications of in situ Hi-C data with a smaller number of chromatin
263 interactions will not be available for this analysis.

264 Promoter capture Hi-C data of NPC was downloaded and analyzed in the same
265 way as T cell and HMEC (Jung et al. 2019). Total 109 biased orientations [61 (28%) FR
266 and 60 (25%) RF of 205 FR and 241 RF] of DNA motif sequences, which included
267 CTCF, cohesin (RAD21 and SMC3), ZNF143 and YY1, showed a significantly higher
268 ratio of EPIs overlapped with promoter capture Hi-C chromatin interactions (≥1 count
269 for each interaction, i.e. all interactions) in EPA (i) than the other types of EPA (ii) and
270 (iii) (Supplemental material). When comparing EPIs predicted based on only EPA (i)
271 and (iii) with the chromatin interactions, total 186 biased orientations [99 (48%) FR and
272 103 (43%) RF of 205 FR and 241 RF] of DNA motif sequences showed a significantly
273 higher ratio of EPIs overlapped with the chromatin interactions in EPA (i) than EPA (iii)
274 (Supplemental material).

All three types of chromatin interaction data (HiChIP, in situ Hi-C and promoter capture Hi-C) indicated that EPIs predicted based on EPA (i) that were shortened at DNA motif sites of known TFs associated with chromatin interactions (CTCF, RAD21, SMC3, ZNF143 and YY1), overlapped with more chromatin interactions than the other EPA (ii) and (iii) in six cell types (T cells, Th17, Treg, GM12878, HMEC and NPC). For monocyte, Hi-C data was available, but it was not analyzed, due to the low resolution of chromatin interaction data (50 kb).

There may be a possibility that the biased orientations of DNA motif sites of known TFs associated with chromatin interactions such as CTCF, RAD21, SMC3, YY1 and ZNF143 are located with the biased orientations of DNA motif sites of other TFs, and thus, they showed a significantly higher ratio of EPIs overlapped with chromatin interactions in EPA (i) than the other types of EPA (ii) and (iii). However, among 273 FR and 211 RF orientations of DNA motifs of TFs not including known TFs such as CTCF, RAD21, SMC3, YY1 and ZNF143 in T cells, the DNA motif sites of only 15 (6%) FR and 9 (4%) RF orientations of DNA motifs of TFs overlapped with $\geq$ 60% of DNA motif sites of biased orientations of DNA motifs of either of the known TFs at 5 kb resolution.

Moreover, to examine the enhancer activity of EPIs, the distribution of expression level of putative target genes of EPIs was compared between EPIs overlapped with HiChIP chromatin interactions and EPIs not overlapped with them. Though the target genes of EPIs were selected from top 4,000 transcripts (genes) in terms of the expression level of all transcripts (genes) excluding transcripts not expressed in T, Th17,

297 Treg and GM12878 cells respectively, target genes of EPIs overlapped with chromatin
298 interactions showed a significantly higher expression level than EPIs not overlapped
299 with them, suggesting that EPIs overlapped with chromatin interactions activated the
300 expression of target genes in the four cell types. Almost all (99% - 100%) FR and RF
301 orientations of DNA motifs showed a significantly higher expression level of putative
302 target genes of EPIs overlapped with chromatin interactions than EPIs not overlapped in
303 the four cell types. When a biased orientation of DNA motif showed a significantly
304 higher expression level of putative target genes of EPIs overlapped with chromatin
305 interactions than EPIs not overlapped, '1' was marked with in the tables of comparison
306 between EPIs and HiChIP chromatin interactions in Supplemental material. DNA motifs
307 showing a significantly lower expression level or not showing a significant difference of
308 expression level were not observed in this analysis. HiChIP data were produced using
309 H3K27ac antibody, so chromatin interactions acting as repressor would not be identified.
310 However, for in situ Hi-C and promoter capture Hi-C data in HMEC and NPC, the
311 significant difference of expression level of putative target genes of EPIs was observed
312 in a small percentage (less than 1%) of biased orientations of DNA motifs.
313
314 **Correlation of expression level of gene pairs separated by DNA motif sites of a TF**
315 To examine the effect of biased orientations of DNA motif sequences on gene
316 expression, I compared the expression level of protein-coding genes the most closely
317 located to upstream and downstream of biased orientations of DNA motif sites in the
318 human genome. Closely located genes including divergent gene pairs are expected to

show correlation of gene expression among tissues (Purmann et al. 2007; Xie et al. 2007). When a biased orientation of DNA motif sites act as insulator (e.g. CTCF), the correlation of gene expression level would be reduced. Among 96 biased (64 FR and 52 RF) orientations of DNA motifs of TFs found in common in monocytes, T cells, HMEC and NPC, TFs with ≥50 genomic locations of the DNA motif sites were selected, after the elimination of ubiquitously expressed genes among 53 tissues and DNA motif sites near the genes with coefficient of variance <90 (see Methods). After this filtering, 43 (72%) FR and 40 (80%) RF of 60 FR and 50 RF showed a distribution of significantly lower correlation of gene expression of the closest genes of the DNA motif sites of a TF than the correlation of all pairs of neighbor genes with intergene distance <1 megabases (Mb) (Mann-Whitney test, p-value < 0.05) (Table 3). The FR and RF orientations of TFs included known TFs associated with chromatin interactions such as CTCF, RAD21, SMC3, YY1 and ZNF143. Top 20 of the FR and RF orientations of DNA motifs were selected in ascending order of the median correlation coefficient of expression level of the closest gene pairs of the DNA motif sites of a TF. The 20 TFs included known TFs associated with chromatin interactions such as CTCF, RAD21 and SMC3 (Fig. 4) (Mann-Whitney test, p-value < 0.01). Instead of using all DNA motif sites of a TF, when DNA motif sites of a TF were limited to sites examined for biased orientations of DNA motifs in EPAs, 33 (60%) FR and 36 (77%) RF of 55 FR and 47 RF showed a distribution of significantly lower correlation of expression level of gene pairs separated by the sites (Supplemental material). With intergene distance <20 kb and TFs with ≥50 genomic locations of the DNA motif sites, 21 (34%) FR and 8 (15%) RF of 62 FR and

52 RF showed a distribution of significantly lower correlation of gene expression of the closest genes of the DNA motif sites of a TF than the correlation of all pairs of neighbor genes (Supplemental material).

Some DNA motif sites of biased orientations of DNA motifs of a TF were found from genomic regions not including known DNA motif sites of TFs associated with chromatin interactions such as CTCF, RAD21, SMC3, YY1 and ZNF143, and were located in genomic regions with significantly lower correlation of expression level of gene pairs. A large number of DNA motif sites of a TF tend to show significantly lower correlation of gene expression (Median numbers of DNA motif sites showing significantly lower correlation were 656 and 479 for FR and RF respectively, and median numbers of DNA motif sites not showing lower correlation were 122 and 115 for FR and RF respectively. Mann-Whitney test p-value = 0 and $< 10^{-10}$ for FR and RF respectively). The DNA motif sites of many TFs showed a significantly lower correlation of gene expression, so there may be a possibility that when we take a small number of gene pairs randomly (about hundreds as the same as the number of DNA motif sites of a TF), the correlation of gene pairs might be significantly low occasionally. However, the possibility that happen was lower than the expectation from p-value threshold by computer simulation.

Co-location of biased orientations of DNA motif sites of TFs

To examine the association of biased orientations of DNA binding motif sequences of TFs, co-location of the DNA binding motif sequences within 200bp to

each other, which is close to the length of core DNA around octamer of core histone (146bp), that is, the length of the minimum open chromatin region, was analyzed in monocytes, T cells, HMEC, and NPC. The same pairs of DNA binding motif sequences in upstream and downstream of genes in EPAs were enumerated, and the pairs of DNA binding motif sequences found in ≥ 100 genomic regions were listed (Table 4; Supplemental material). Majority of pairs of DNA motif sites overlapped with more than 1 base, but the same tendency was found in the analysis of DNA motif sites of all TFs (Supplemental material). As already known, CTCF was found with cohesin RAD21 and SMC3 (Table 4). Top 30 pairs of FR and RF orientations of DNA motifs overlapped or co-localized were shown (Table 4). Total numbers of unique pairs of DNA motif sites of TFs overlapped or co-localized were 404 (FR) and 662 (RF) in monocytes, consisting of 177 (39% of all FR) and 218 (43% of all RF) unique DNA motifs. Only ten overlapping or co-location of DNA motifs of TFs were found in the four cell types in common, including pairs of CTCF, RAD21, SMC3 and YY1. This implied that most of overlapping and co-location of DNA motifs of TFs act in cell-type-specific manner (Supplemental material). Pairs of biased orientations of DNA binding motifs of TFs tend to overlap, and relatively a small number of motifs are co-localized in upstream and downstream of genes. Overlapping DNA motifs act as DNA binding sites of several TFs simultaneously or competitively (Ackerman et al. 1991; Yoon and Chikaraishi 1992; Ansari and Peterson-Kaufman 2011; Slattery et al. 2011; Chatterjee et al. 2012; He et al. 2015; Kin et al. 2016; Merabet and Mann 2016). CTCF and cohesin have also been reported to act coordinately with another TF and a protein such as Klf4 and Brd2

(Wei et al. 2013; Hsu et al. 2017). Klf4 recruits cohesin to the Oct4 enhancer region. BRD2 supports boundary (insulator) activity of CTCF. The analysis of 457 ChIP-seq data sets on 119 human TFs showed that secondary motifs were detected in addition to the canonical motifs of the TFs, indicating tethered binding and co-binding between multiple TFs (Wang et al. 2012a). The authors observed significant position and orientation preferences between many co-binding TFs. Overlapping DNA motif sites of TFs found in this study may not be artifact, but biologically functional. Though repeat sequences in human genome were masked, more than a hundred of pairs of DNA motif sites overlapped at hundreds or thousands upstream and downstream regions of genes.

Discussion

To find DNA motif sequences of transcription factors (TFs) affecting the expression level of human putative transcriptional target genes, DNA motif sequences were searched from open chromatin regions of monocytes, T cells, HMEC and NPC. Total 96 biased [64 forward-reverse (FR) and 52 reverse-forward (RF)] orientations of DNA motif sequences of TFs were found in the four cell types in common, whereas any orientation (i.e. without considering orientation) of DNA motif sequence of a TF was not found to affect the expression level of putative transcriptional target genes, suggesting that an enhancer-promoter association (EPA) shortened at the FR or RF orientation of DNA motif sites of a TF includes more accurate prediction of enhancer-promoter interactions (EPIs), which were supported by the comparisons with chromatin interaction and gene expression data..

In general, DNA motif sequences of TFs were searched from genome sequences using position weight matrix or position frequency matrix and allowing mismatches of DNA sequences under a certain threshold. However, the change of the threshold affected the result of analyses, and it seems to be difficult to find the best parameter setting to reduce false-positive and false-negative predictions of DNA biding sites of TFs. Therefore, firstly, to obtain a robust result in this study, position weight matrixes of DNA motifs were converted into consensus DNA sequences including degenerated sites, which consist of alphabet of 15 characters (See Methods). This does not need parameter setting in the search for DNA motif sequences, and is the same as *k*-mer analysis of DNA motif sequences of TFs. Thought the number of genomic regions matched with a DNA motif sequence was decreased, about 200 FR and RF orientations of DNA motif sequences of TFs were found, and the number of any orientation of DNA motif sequences of TFs was quite small, suggesting that false-positive prediction of DNA biding sites of TFs was reduced. However, the length of the consensus DNA sequences of some TFs is relatively long. When the core DNA binding sequence of a TF is short (5 or 6 bp), it may be strict to find perfect matches of long consensus DNA sequences in genome sequences, not allowing a mismatch of the DNA sequence (Methods in (Xie et al. 2007)).

Secondly, protein interaction quantitation (PIQ) tool was used to find DNA motif sites of TFs (Sherwood et al. 2014). PIQ predicts DNA motif sites of TFs by reducing noises of DNase-seq data, and the comparison of the prediction with ChIP-seq data revealed that PIQ has a better performance than other tools and digital genome

429 footprinting (DNase-DGF). The prediction of DNA motif sites of TFs using PIQ in this
430 study showed an increase of biased orientations of DNA motif sequences of TFs,
431 reducing the number of any orientation of DNA motif sequences of TFs. The number of
432 DNA motif sites of TFs was expected to increase, relative to the above method to use
433 consensus DNA sequences of TFs in the preceding section. However, the number of
434 DNA motif sites was almost the same or slightly decreased, compared with the result of
435 consensus DNA sequences, suggesting that PIQ increases true positive predictions of
436 DNA motif sites, reducing false positive predictions.

437 To estimate the enhancer activity of DNA motifs of TFs, the expression level of
438 putative transcriptional target genes of a TF was compared between DNA motif sites of
439 TFs in distal open chromatin regions (enhancers) and closed chromatin regions in
440 promoters. Previously, the expression level was compared between distal open
441 chromatin regions and open chromatin regions in promoters. However, it would be easy
442 to understand the comparison of DNA motif sites of a TF between distal open chromatin
443 regions and closed chromatin regions to estimate the enhancer activity of TFs. The
444 number of DNA motif sites in closed chromatin regions was large, so the number in
445 closed chromatin regions in promoter was used.

446 When forming a homodimer or heterodimer with another TF, TFs may bind to
447 genome DNA with a specific orientation of their DNA binding sequences (Fig. 5). From
448 the analysis of biased orientations of DNA motif sequences of TFs, TFs forming
449 heterodimer would also be found. If the DNA binding motif sequence of only the mate
450 to a pair of TFs was found in an EPA, the EPA was shortened at one side, which is the

451 DNA binding motif site of the mate to the pair, and transcriptional target genes were
452 predicted using the EPA shortened at the side. In this analysis, the mate to both
453 heterodimer and homodimer of TFs can be used to examine the effect on the expression
454 level of transcriptional target genes predicted based on the EPA shortened at one side.
455 Biased orientations of DNA motif sequences may also be found in forward-forward or
456 reverse-reverse orientation.

457 At first, EPIs were compared with chromatin interactions (Hi-C) in monocytes.
458 Using open chromatin regions overlapped with peaks of ChIP-seq experiment of histone
459 modification marks of an enhancer (H3K27ac), the ratio of EPIs not overlapped with
460 chromatin interactions was reduced. (Phanstiel et al. 2017) also reported that there was
461 an especially strong enrichment for loops with H3K27 acetylation peaks at both ends
462 (Fisher's Exact Test, $p = 1.4 \times 10^{-27}$). However, the total number of EPIs overlapped
463 with chromatin interactions was also reduced using H3K27ac peaks, so more chromatin
464 interaction data would be needed to obtain reliable results in this analysis. As an issue of
465 experimental data, data for chromatin interactions and open chromatin regions were
466 obtained from different samples and donors, so individual differences would exist. The
467 resolution of chromatin interaction data used in monocytes was about 50 kb, thus the
468 number of unique chromatin interactions was relatively small (72,284 at 50 kb
469 resolution with a cutoff score of CHiCAGO tool > 1 and 16,501 with a cutoff score of
470 CHiCAGO tool > 5) ('PCHiC_peak_matrix_cutoff0.txt.gz' file was downloaded from
471 'Promoter Capture Hi-C in 17 human primary blood cell types' website
472 https://osf.io/u8tzp/files/). To examine the difference of the numbers of EPIs overlapped

473 with chromatin interactions, according to the three types of EPAs, the unique and total
474 number of chromatin interactions should be large enough.

475 As HiChIP chromatin interaction data were available in $CD4^+$ T, Th17, Treg and
476 GM12878 cells, biased orientations of DNA motif sequences of TFs were examined in
477 the four cell types. The resolutions of chromatin interactions and EPIs were adjusted to
478 5 kb by fragmentation of genome sequences. The number of unique HiChIP cis (i.e. in
479 the same chromatin) chromatin interactions was 19,926,360 at 5 kb resolution in B2T1
480 replication of T cells, 666,149 at 5 kb resolution with chromatin interactions (≥1,000
481 counts for each interaction) and 78,209 at 5 kb resolution with chromatin interactions
482 (≥6,000 counts for each interaction) (Supplemental material). As expected, the number
483 of EPIs overlapped with chromatin interactions was increased, and 133 FR and 90 RF
484 orientations of DNA motif sequences of TFs showed a statistical significance in EPIs
485 predicted based on an EPA shortened at the DNA motif sites of TFs, compared with the
486 other types of EPA or EPA not shortened. The numbers of unique HiChIP cis chromatin
487 interactions in other cell types (Th17, Treg and GM12878) were shown in Supplemental
488 material. The numbers of unique cis chromatin interactions at 5 kb resolution were
489 different among replications in Th17 cells, so the numbers of interactions were adjusted
490 between the numbers with ≥1,000 and ≥6,000 counts for each interaction in T cells.
491 For Treg, chromatin interactions in one biological replication overlapped with EPIs, but
492 those in the other two biological replications were less overlapped with EPIs, so the one
493 replication was used for this analysis. HiChIP analysis used H3K27ac antibody to
494 capture chromatin interactions and identified twenty millions of chromatin interactions,

but the number of peaks of ChIP-seq experimental data of H3K27ac is usually less than a hundred thousand. There seems to be much difference of the number of H3K27ac sites between HiChIP and ChIP-seq, so ChIP-seq peaks of H3K27ac may not cover all H3K27ac sites. For HMEC, in situ Hi-C chromatin interaction data were available, the number of unique in situ Hi-C cis chromatin interactions was 121,873,642 at 3 kb resolution. All chromatin interaction data were used for this analysis to compare EPIs with chromatin interactions. For NPC, the number of unique promoter capture Hi-C cis chromatin interactions was 9,436,689 at 5 kb resolution. All chromatin interaction data were utilized for analysis.

It has been reported that CTCF and cohesin-binding sites are frequently mutated in cancer (Katainen et al. 2015). Some biased orientations of DNA motif sequences would be associated with chromatin interactions and might be associated with diseases including cancer.

The analyses in this study revealed properties of DNA binding motif sequences of TFs involved in chromatin interaction, insulator function and potentially forming a homodimer, heterodimer or complex with other TFs, affecting the transcriptional regulation of genes.

Methods

Search for biased orientations of DNA motif sequences

To identify transcription factor binding sites (TFBSs) from open and closed chromatin regions, TRANSFAC (2019.2), JASPAR (2018), UniPROBE (2018),

517 high-throughput SELEX, transcription factor binding sequences of ENCODE ChIP-seq
518 data, and HOCOMOCO version 9 and 11 were used to predict insulator sites
519 (Wingender et al. 1996; Newburger and Bulyk 2009; Portales-Casamar et al. 2010; Xie
520 et al. 2010; Zhao and Stormo 2011; Jolma et al. 2013; Kheradpour and Kellis 2014;
521 Kulakovskiy et al. 2018). TRANSFAC (2019.2) was used to analyze enhancer-promoter
522 interactions, because these data were sufficient to identify biased orientations of DNA
523 motif sequences of insulator TFs with less computational time, reducing the number of
524 any orientation of DNA motif sequences of TFs. To reduce false positive prediction of
525 DNA motif sites of TFs in open chromatin regions, protein interaction quantitation
526 (PIQ) tool was used with 12,249 position frequency matrices converted from DNA
527 motifs of vertebrate TFs in the above databases and DNase-seq data from GEO and
528 Encode database (GSM1024791 $CD14^+$ monocytes; GSM665812 $CD4^+$ T cell;
529 GSM736634 Human mammary epithelial cell, HMEC; GSM878615 Neural progenitor
530 cell, NPC; ENCFF263GMV, ENCFF886XEV Th17; GSM1024741 Treg; GSM736620
531 GM12878) (Sherwood et al. 2014). To find open chromatin regions associated with
532 enhancer (and promoter) activity, ChIP-seq experimental data of H3K27ac was
533 downloaded (GSM773004). Narrow peaks of ChIP-seq data were predicted using macs2
534 callpeak (Zhang et al. 2008). To predict DNA motif sites of TFs from closed chromatin
535 regions, another method was used. Position weight matrices of vertebrate transcription
536 factor binding sequences were converted into DNA consensus sequences, which
537 consist of alphabet of 15 characters (the four bases A, C, G, T, the six two-fold
538 degenerate IUPAC codes R=[AG], Y=[CT], K=[GT], M=[AC], S=[GC], W=[AT], the

four three-fold degenerate IUPAC codes B=[CGT], D=[AGT], H=[ACT], V=[ACG], and the four-fold degenerate character N=[ATGC]) using convert matrix in RSAT website (van Helden 2003). Transcription factor binding sequences of vertebrate TFs were used for further analyses. Transcription factor binding sequences were searched from narrow peaks of DNase-seq data in repeat-masked hg19 genome sequences using Match tool in TRANSFAC with similarity score cutoff of 1 after transforming the DNA consensus sequences of TFs into position frequency matrixes for Match search (Kel et al. 2003). Repeat-masked hg19 genome sequences were downloaded from UCSC genome browser (http://genome.ucsc.edu/, http://hgdownload.soe.ucsc.edu/goldenPath/hg19/bigZips/hg19.fa.masked.gz). TFs corresponding to transcription factor binding sequences were searched computationally and manually by comparing their names and gene symbols of HGNC (HUGO Gene Nomenclature Committee) -approved gene nomenclature and 31,848 UCSC known canonical transcripts (http://hgdownload.soe.ucsc.edu/goldenPath/hg19/database/knownCanonical.txt.gz), as transcription factor binding sequences were not linked to transcript IDs such as UCSC, RefSeq and Ensembl transcripts.

Target genes of a TF were assigned when its TFBS was found in DNase-seq narrow peaks in promoter or extended regions for enhancer-promoter association of genes (EPA). Promoter and extended regions were defined as follows: promoter regions were those that were within distance of ±5 kb from transcriptional start sites (TSS). Promoter and extended regions were defined as per the following association rule,

561 which is the same as that defined in Figure 3A of a previous study (McLean et al. 2010):
562 the single nearest gene association rule, which extends the regulatory domain to the
563 midpoint between the TSS of the gene and that of the nearest gene upstream and
564 downstream without the limitation of extension length. Extended regions for EPA were
565 shortened at the DNA binding sites of a TF that was the closest to a TSS, and
566 transcriptional target genes were predicted from the shortened enhancer regions using
567 TFBS. Furthermore, promoter and extended regions for EPA were shortened at the
568 forward–reverse (FR) orientation of DNA binding sites of a TF. When forward or
569 reverse orientation of DNA binding sites were continuously located in genome
570 sequences several times, the most internal (i.e. closest to a TSS) forward–reverse
571 orientation of DNA binding sites were selected. The genomic positions of genes were
572 identified using 'knownGene.txt.gz' file in UCSC bioinformatics sites (Karolchik et al.
573 2014). The file 'knownCanonical.txt.gz' was also utilized for selecting representative
574 transcripts among various alternate forms for assigning promoter and extended regions
575 for EPA. From the list of transcription factor binding sequences and transcriptional
576 target genes, redundant transcription factor binding sequences were removed by
577 comparing the target genes of a transcription factor binding sequence and its
578 corresponding TF; if identical, one of the transcription factor binding sequences was
579 used. When the number of transcriptional target genes predicted from a transcription
580 factor binding sequence was less than five, the transcription factor binding sequence
581 was omitted.

582 Repeat DNA sequences were searched from hg19 version of the human reference

583 genome using RepeatMasker (Smit, AFA & Green, P RepeatMasker at
584 http://www.repeatmasker.org) and RepBase RepeatMasker Edition
585 (http://www.girinst.org).

586 For gene expression data, RNA-seq reads mapped onto human hg19 genome
587 sequences were obtained from UCSF-UBC human reference epigenome mapping
588 project RNA-seq reads with poly-A of naive $CD4^+$ T cells (GEO: GSM669617).
589 RNA-seq reads were aligned in repeat-masked hg19 genome sequences using BWA
590 with default parameters (Li and Durbin 2009). FPKMs of the RNA-seq data were
591 calculated using RSeQC (Wang et al. 2012b). For monocytes, Blueprint RNA-seq
592 FPKM data
593 ('C0010KB1.transcript_quantification.rsem_grape2_crg.GRCh38.20150622.results')
594 were downloaded from Blueprint DCC portal
595 (http://dcc.blueprint-epigenome.eu/#/files). RNA-seq reads with poly-A of human
596 mammary epithelial cells (HMEC) in Encyclopedia of DNA Elements at UCSC
597 (http://genome.ucsc.edu/encode/,
598 'wgEncodeCshlLongRnaSeqHmecCellPapAlnRep1.bam' file), H1 derived neural
599 progenitor cell (NPC) (GEO: GSM915326, ENCODE: ENCFF529SIO), Th17
600 (GSM2859479, NCBI SRA: SRR6298326), Treg (GSM2859476, SRR6298323) and
601 GM12878 (GSE78551, ENCFF297QCE) were used. Based on log2-transformed FPKM,
602 UCSC transcripts were arranged in descending order of expression level, and top 4,000
603 transcripts were selected in each cell type.

604 The expression level of transcriptional target genes predicted based on EPAs

605 shortened at the DNA motif sites of a TF was compared with the expression level of
606 transcriptional target genes predicted from closed chromatin regions in promoters. For
607 each DNA motif sequence shortening EPAs, transcriptional target genes were predicted
608 using DNA binding motif sequences of vertebrate TFs in TRANSFAC database, and the
609 ratio of expression level of putative transcriptional target genes of each TF was
610 calculated between EPAs and closed chromatin regions in promoters. The distribution of
611 the ratios of all TFs was compared among forward-reverse (FR), reverse-forward (RF)
612 and any orientation (i.e. without considering orientation) of a DNA motif sequence
613 shortening EPAs using Mann-Whitney test, two-sided (p-value $< 10^{-7}$). Other
614 parameters for the analysis were that the number of transcriptional target genes of a TF
615 was $\geq$50, and the number of general TFs (not insulator TFs) to predict transcriptional
616 target genes was $\geq$50. The number of DNA motif sites of a TF (insulator TF)
617 shortening EPAs was $\geq$100.
618
619 **Comparison with chromatin interaction data**
620 For comparison of EPIs with chromatin interactions (HiChIP) in $CD4^+$ T, Th17,
621 Treg and GM12878 cells,
622 'GSM2705049_Naive_HiChIP_H3K27ac_B2T1_allValidPairs.txt',
623 'GSM2705050_Naive_HiChIP_H3K27ac_B2T2_allValidPairs.txt',
624 'GSM2705051_Naive_HiChIP_H3K27ac_B3T1_allValidPairs.txt',
625 'GSM2705054_Th17_HiChIP_H3K27ac_B1T2_allValidPairs.txt',
626 'GSM2705055_Th17_HiChIP_H3K27ac_B2T1_allValidPairs.txt',

627 'GSM2705056_Th17_HiChIP_H3K27ac_B3T1_allValidPairs.txt',
628 'GSM2705059_Treg_HiChIP_H3K27ac_B3T1_allValidPairs.txt',
629 'GSM2705041_GM_HiChIP_H3K27ac_B1_allValidPairs.txt',
630 'GSM2705042_GM_HiChIP_H3K27ac_B2_allValidPairs.txt' files were downloaded
631 from Gene Expression Omnibus (GEO) database. The resolutions of chromatin
632 interactions and EPIs were adjusted to 5 kb before their comparison. Chromatin
633 interactions with ≥6,000 and ≥1,000 counts for each interaction were used in $CD4^+$ T
634 cells. According to the unique numbers of chromatin interactions in replications in Th17,
635 Treg and GM12878 cells, chromatin interactions with ≥1,000 (B1T2 in Th17),
636 ≥2,000 (B2T1 and B3T1 in Th17), ≥6,000 (B3T1 in Treg), ≥4,000 (B1 and B2 in
637 GM12878) counts for each interaction were analyzed.

638 Enhancer-promoter interactions (EPIs) were predicted using three types of EPAs
639 in monocytes: (i) EPA shortened at the FR or RF orientation of DNA motif sites of a TF,
640 (ii) EPA shortened at the any orientation (i.e. without considering orientation) of DNA
641 motif sites of a TF, and (iii) EPA without being shortened by a DNA motif site. EPIs
642 predicted in the three types of EPAs in common were removed. EPIs predicted from
643 EPA (i) were removed from EPIs predicted from EPA (ii). EPIs predicted from EPA (i)
644 and (ii) were removed from EPIs predicted from EPA (iii). The resolution of HiChIP
645 chromatin interaction data was 1-5 kb, so EPIs were adjusted to 5 kb before their
646 comparison. The number and ratio of EPIs overlapped with chromatin interactions were
647 compared two times between EPIs (i) and (iii), and EPIs (i) and (ii) (binomial
648 distribution, p-value < 0.025 for each test, two-sided, 95% confidence interval).

649 For comparison of EPIs with chromatin interactions (in situ Hi-C) in HMEC,
650 'HMEC_4DNFI97O9SAZ.pairs.gz' file was downloaded from 4D nucleome data portal
651 (http://data.4dnucleome.org). The genomic positions of chromatin interactions were
652 converted into hg19 version of human genome using liftOver tool
653 (http://hgdownload.soe.ucsc.edu/downloads.html#liftover). The resolutions of
654 chromatin interaction data and EPIs were adjusted to 3 kb before their comparison. All
655 chromatin interactions were used for analysis. For comparison of EPIs with chromatin
656 interactions (promoter capture Hi-C) in NPC, 'GSE86189_npc.po.all.txt.bz2' file was
657 downloaded from GEO database (GSE86189). The resolutions of chromatin interaction
658 data and EPIs were adjusted to 5 kb before their comparison. All chromatin interactions
659 were used for analysis.

660 Putative target genes for the comparison of EPIs and chromatin interactions were
661 selected from top 4,000 transcripts in term of the expression level. The expression level
662 of putative target genes of EPIs overlapped with chromatin interactions was compared
663 with EPIs not overlapped with them. When a putative transcriptional target gene of a TF
664 in an enhancer was found in both an EPI overlapped with a chromatin interaction and an
665 EPI not overlapped with, the target gene was eliminated. The distribution of expression
666 level of putative target genes was compared using Mann-Whitney test, two-sided
667 (p-value < 0.05).

668

669 **Correlation of expression level of gene pairs separated by DNA motif sites of a TF**

670 To examine the correlation of expression level of genes pairs separated by DNA

motif sites of a TF, gene expression data among 53 tissues were obtained from 'GTEx_Analysis_2016-01-15_v7_RNASeQCv1.1.8_gene_median_tpm.gct.gz' file in GTEx database (https://gtexportal.org/home/). The correlation of log2-transformed gene expression level was analyzed based on protein-coding transcripts of RefSeq (RefSeq ID with 'NM_'). The same genomic location of RefSeq transcripts were removed. DNA motif sites overlapped with RefSeq transcripts were eliminated. Genes closest to a DNA motif sites and another gene were analyzed using BEDOPS closest-features (Neph et al. 2012). Mann-Whitney test was performed using R.

Co-location of biased orientations of DNA motif sites of TFs

Co-location of biased orientations of DNA binding motif sites of TFs was examined. The number of genomic regions with the same pair of biased orientations of DNA motifs of TFs in upstream and downstream of genes in EPAs was counted, and the same pair of DNA motif sites of TFs found in ≥100 genomic regions was listed.

Acknowledgements

The supercomputing resource was provided by Human Genome Center of the Institute of Medical Science at the University of Tokyo. Computations were partially performed on the NIG supercomputer at ROIS National Institute of Genetics. Publication charges for this article were funded by JSPS KAKENHI Grant Number 16K00387. This research was partially supported by the Platform Project for Supporting in Drug Discovery and Life Science Research（Platform for Dynamic Approaches to Living

693 System）from Japan Agency for Medical Research and Development (AMED). This
694 research was partially supported by Development of Fundamental Technologies for
695 Diagnosis and Therapy Based upon Epigenome Analysis from Japan Agency for
696 Medical Research and Development (AMED). This work was partially supported by
697 JST CREST Grant Number JPMJCR15G1, Japan.
698

Figures

Web links to original figures.

Figure 1. (A) Figure 1. Enhancers and their features. (Shlyueva et al. 2014)

https://static-content.springer.com/esm/art%3A10.1038%2Fnrg3682/MediaObjects/41576_2014_BFnrg3682_MOESM18_ESM.ppt

Graphical Abstract (de Wit et al. 2015)

https://marlin-prod.literatumonline.com/cms/attachment/7d219941-8398-4373-9ac9-8bf92c5eba1d/fx1.jpg

(B) Supplementary Figure 2. Computationally-defined regulatory domain (McLean et al. 2010)

https://static-content.springer.com/esm/art%3A10.1038%2Fnbt.1630/MediaObjects/41587_2010_BFnbt1630_MOESM11_ESM.pdf

Figure 4. The Role of CBS Location and Orientation in CTCF-Mediated Genome-wide DNA Looping (Guo et al. 2015)

https://marlin-prod.literatumonline.com/cms/attachment/297a06ad-7568-483e-9904-9ae2af081251/gr4.jpg

Figure 1. Chromatin interaction and enhancer-promoter association. (A) Forward–reverse orientation of CTCF-binding sites are frequently found in chromatin interaction anchors. CTCF can block the interaction between enhancers and promoters limiting the activity of enhancers to certain functional domains (Rao et al. 2014; Shlyueva et al.

721 2014; de Wit et al. 2015; Guo et al. 2015). (B) Computationally-defined regulatory
722 domains for enhancer-promoter association (McLean et al. 2010). The *single nearest*
723 *gene* association rule extends the regulatory domain to the midpoint between this gene's
724 TSS and the nearest gene's TSS both upstream and downstream. Enhancer-promoter
725 association was shortened at the forward-reverse orientation of DNA binding motif sites
726 of a transcription factor in this study (e.g. CTCF in the figure).
727

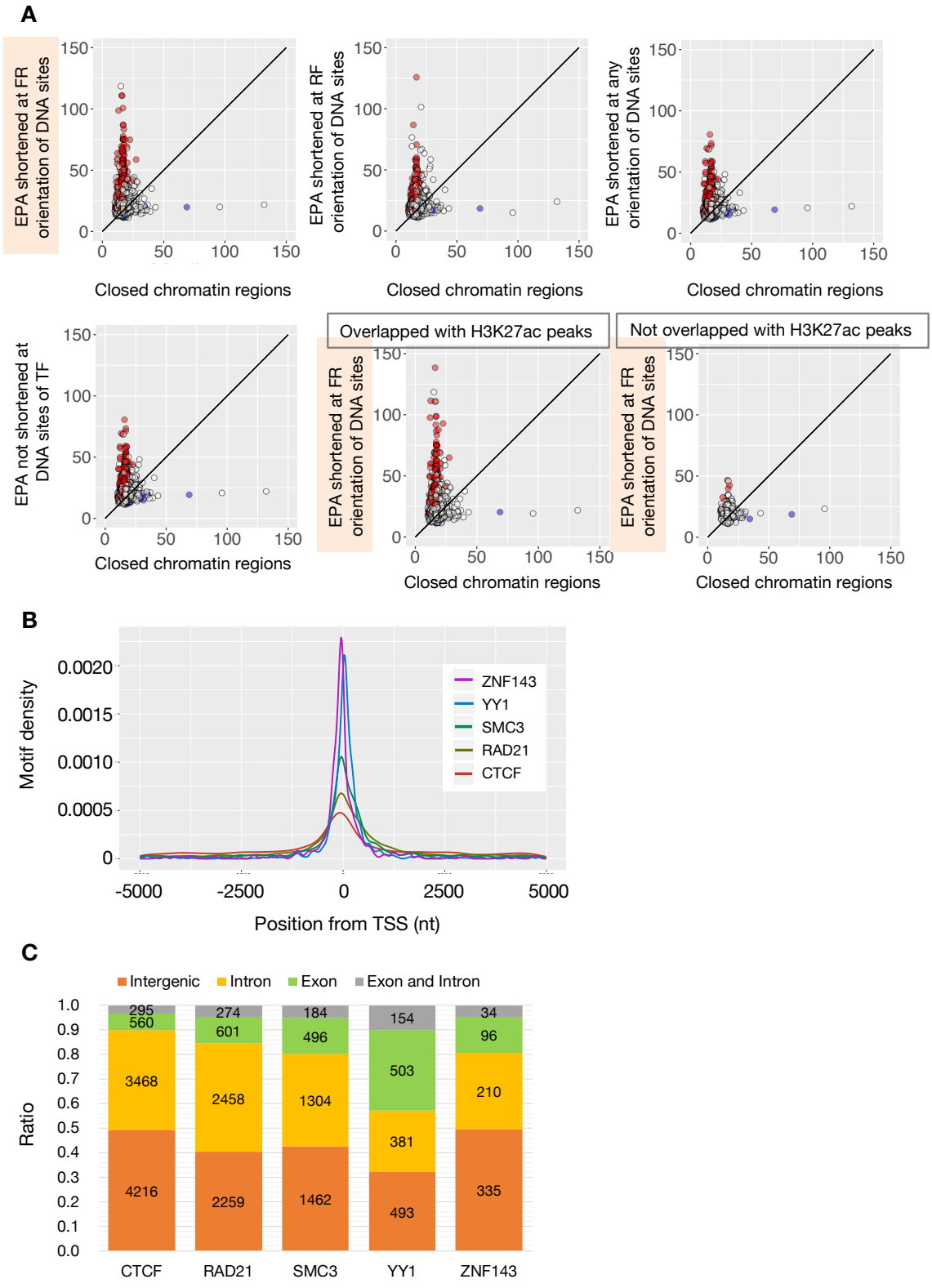

Figure 2. Identification of DNA motif sites of TFs from open chromatin regions and properties of DNA motif sites of TFs. (A) Comparison of expression level of putative

731 transcriptional target genes. Each dot shows the median expression level (FPKM) of
732 target genes predicted from DNA sites of a transcription factor in closed chromatin
733 regions (or promoters) (X-axis) and enhancer-promoter association (EPA) shortened at
734 the forward-reverse orientation of DNA motif sites of CTCF (Y-axis) in T cell (upper
735 left graph). The distribution of expression level was changed according to four criteria
736 of EPAs (four graphs) (see Method) (Osato 2018). Red dots show the median expression
737 level of target genes was significantly higher in EPA than closed chromatin regions, and
738 blue dots show the median expression level of target genes was significantly lower in
739 EPA than closed chromatin regions (Mann-Whitney test). The expression level of target
740 genes predicted in EPA tend to be higher than closed chromatin regions, implying that
741 TFs acted as activators of target genes. DNA motif sites of TFs overlapped with
742 H3K27ac ChIP-seq peaks showed significant differences of expression level of target
743 genes, and DNA motif sites not overlapped with H3K27ac peaks did not show the
744 difference (lower right two graphs). This suggested that the significant differences of
745 expression level were associated with enhancer (and promoter) signals of H3K27ac. (B)
746 Distribution of DNA motif sites of TFs near TSS. ZNF143 and YY1 tend to be located
747 near TSS, and CTCF tend to be observed more from distant regions than around TSS in
748 monocyte. (C) Distribution of DNA motif sites of TFs in the human genome in
749 monocytes. Most of DNA motif sites were found from intergenic and intron regions.
750 YY1 is known to be at TSS in the edge of exons of genes, and is associated with
751 transcriptional activation, repression and initiation. YY1 is multi-functional
752 transcriptional regulator (Shrivastava and Calame 1994; Xi et al. 2007)

753

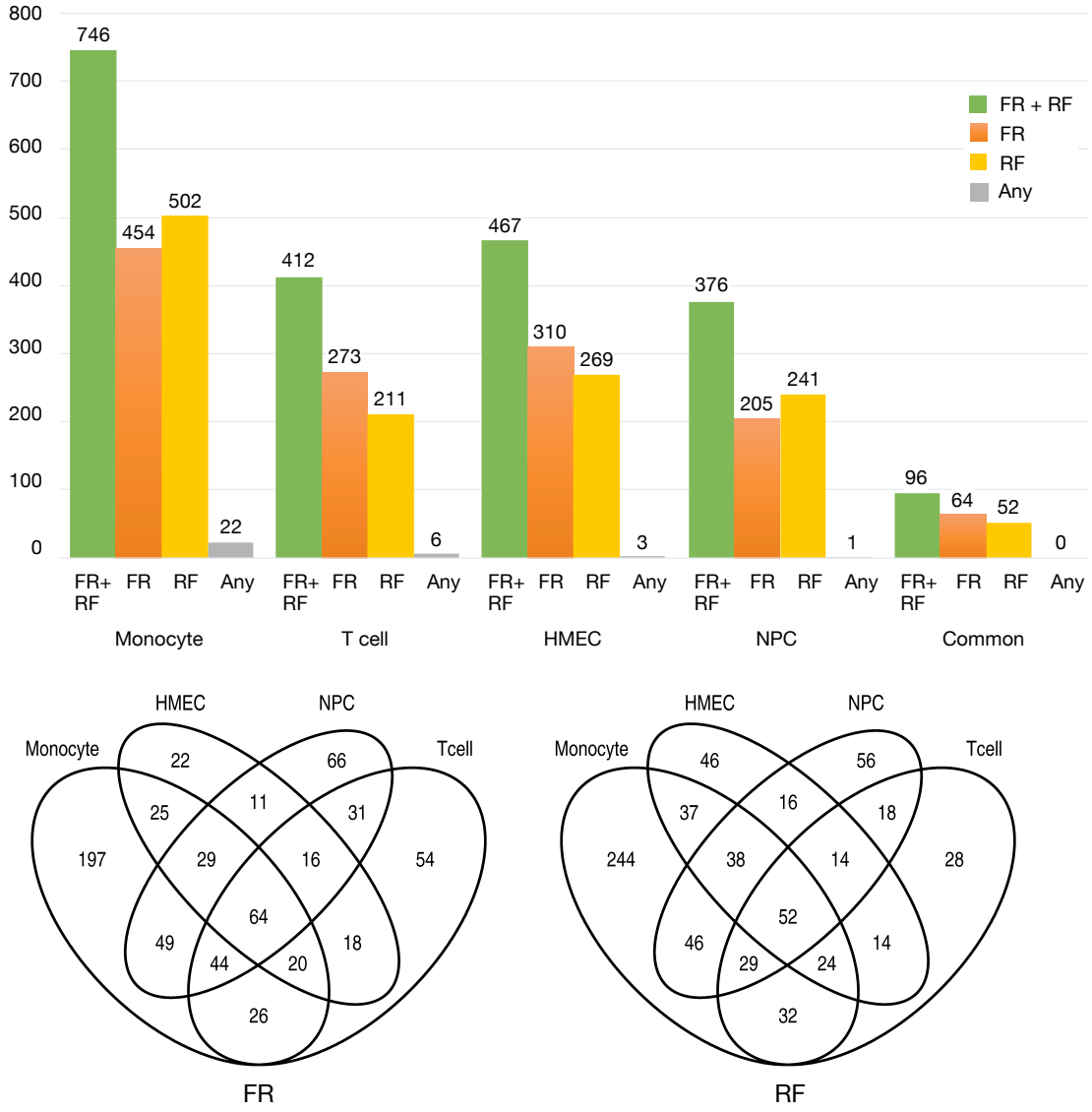

754

755 **Figure 3.** Biased orientations of DNA motif sequences of TFs affecting the transcription
756 of genes by putative insulator function of the DNA motif sites. Total 96 (64 FR and 52
757 RF) of biased orientations of DNA binding motif sequences of TFs were found to affect
758 significantly the expression level of putative transcriptional target genes in monocytes,
759 T cells, HMEC and NPC in common, whereas any orientation (i.e. without considering

760 orientation) of DNA binding motif sequence of a TF was not found to affect the
761 expression level significantly.
762

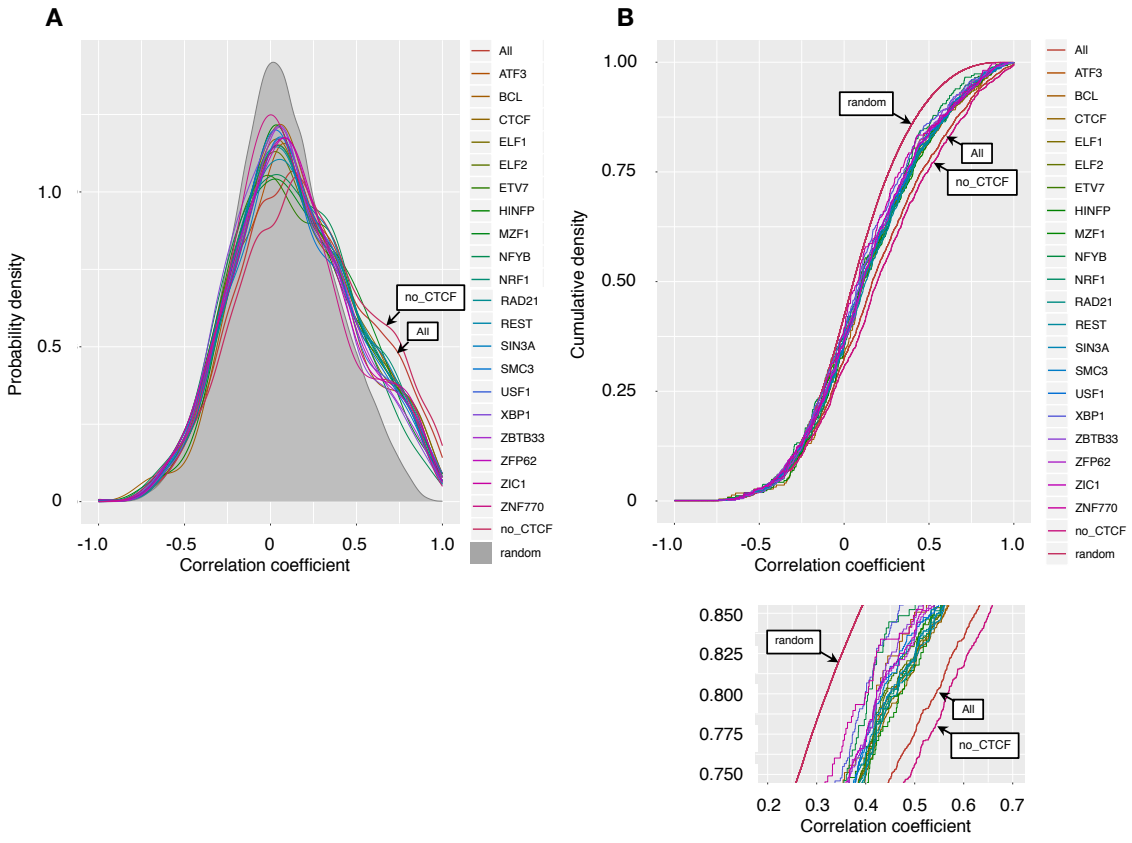

763

764 **Figure 4.** Genes separated by predicted DNA binding sites of biased orientations of
765 DNA motifs of TFs are less correlated in gene expression. Top 20 TFs are shown
766 according to ascending order of median correlation coefficient. Correlation coefficient
767 between neighboring gene pairs is shown in terms of probability density (A) and
768 cumulative distribution (B). Brown line (All), correlation between all neighboring
769 genes; gray shading in (A) and red line (random) in (B), correlation between randomly
770 chosen gene pairs; Purple line (no_CTCF), correlation between gene pairs not separated
771 by predicted CTCF sites.

772 Web links to original figures.

773 Figure 5. Schematic representation of chromatin interactions involving gene promoters

774 (Bailey et al. 2015).

775 https://www.nature.com/articles/ncomms7186/figures/5

776

777 **Figure 5.** Schematic representation of chromatin interactions involving gene promoters.

778 ZNF143 contributes the formation of chromatin interactions by directly binding the

779 promoter of genes establishing looping with distal element bound by CTCF (Bailey et al.

780 2015).

781

782

Tables

Table 1. Biased orientations of DNA binding motif sequences of TFs in monocytes, T cells, HMEC and NPC. TF: DNA binding motif sequences of transcription factors.

Forward-reverse orientation

TF	P-value
AHR	0
ARNT	0
ARNTL	7.96E-08
ATF2	3.09E-14
ATF3	2.22E-15
BCL	0
BHLHE41	5.55E-14
CREB3L1	0
CTCF	0
CXXC1	0
E2F	0
E2F1	0
EGR1	0
EGR3	0
EGR4	0
ELF1	0
ELF2	5.74E-13
ELK3	3.33E-15
ELK4	6.19E-11
ERG	0
ETS	0
ETS1	0
ETV7	2.31E-08
HEY2	0
HIC1	0
HINFP	6.46E-14
INSM1	2.22E-16
KLF4	0
KLF7	9.07E-09
MAX	0

TF	P-value
MYC	0
MYCN	0
MZF1	0
NFY	1.72E-11
NFYB	0
NONO	0
NRF1	1.63E-11
OVOL2	0
PLAG1	0
PLAGL1	0
RAD21	0
REST	0
RFX1	0
SIN3A	0
SIX5	0
SMC3	0
SP2	1.04E-11
TFAP2A	0
TFAP2B	2.22E-16
TFAP2C	0
TP73	0
USF1	0
XBP1	0
YY1	0
YY2	0
ZBTB33	0
ZBTB7A	0
ZFP62	0
ZFX	0
ZIC1	0

TF	P-value
ZNF143	0
ZNF740	0
ZNF770	6.51E-08
ZNF84	0

Reverse-forward orientation

TF	P-value
AP1	0
ARNT	1.26E-11
ATF3	0
BHLHE40	8.88E-16
CREB1	0
CTCF	0
E2F	2.32E-13
E2F3	0
EFNA2	6.61E-11
EGR1	0
EGR2	0
ETS1	0
FLI1	1.05E-13
FLI1:FIGLA	0
FOS	0
GMEB2	0
HIF1A	0
KLF4	0
MITF	0
MYB	0
MYC	0
MYCN	0
MZF1	0
NFKB1	0
NFYA	2.31E-13
NR3C1	0
NRF1	0
OSR2	0
PBX3	0
PLAG1	2.78E-14

TF	P-value
RFX2	0
RFX5	0
RUNX3	0
SP1	0
SP2	0
SP4	0
SPDEF	0
SREBF2	0
STAT	0
TATA	0
TFAP2B	2.00E-15
TFAP2C	0
TFCP2L1	0
USF1	7.55E-10
YBX1	0
YY1	0
YY2	0
ZBTB33	0
ZBTB7B	0
ZNF100	6.22E-14
ZNF143	0
ZNF432	0

790 **Table 2.** Comparison of enhancer-promoter interactions (EPIs) with chromatin
791 interactions in T cells. The upper tables show the number of biased orientations of DNA
792 motifs, where a significantly higher ratio of EPIs predicted based on enhancer-promoter
793 association (EPA) (i) overlapped with HiChIP chromatin interactions than the other
794 types of EPA (ii) and (iii). The middle tables show 133 FR and 90 RF orientations of
795 DNA motifs in T cells found in common among B2T1, B2T2 and B3T1 replications in
796 the upper table. The lower tables show that among 64 FR and 52 RF biased orientations
797 of DNA motifs found in common in monocytes, T cell, HMEC and NPC, 44 (69%) FR
798 and 28 (54%) RF were matched with the analysis of HiChIP chromatin interactions for
799 three types of EPAs. TF: DNA binding motif sequence of a transcription factor. Score: –
800 $\log_{10}$ (*p*-value). Score 1: Comparison of EPAs shortened at the FR or RF orientation of
801 DNA motif sites [EPA (i)] with EPA not shortened [EPA (iii)]. Score 2: Comparison of
802 EPAs shortened at the FR or RF orientation of DNA motif sites [EPA (i)] with EPAs
803 shortened at the any orientation of DNA motif sites [EPA (ii)].

1. Comparison of EPI with HiChIP data among three EPA (i), (ii) and (iii)

Replication of HiChIP data	Total no. (FR + RF) of DNA motifs	No. of FR DNA motifs	No. of RF DNA motifs
B2T1	226	153	101
B2T2	221	149	98
B3T1	237	160	109
DNA motifs found in common among replications			
B2T1 and B2T2	212	141	95
B2T1 and B3T1	212	143	93
B2T2 and B3T1	208	138	93
B2T1, B2T2 and B3T1	201	133	90

2. Comparison of EPI with HiChIP data between two EPA (i) and (iii)

Replication of HiChIP data	Total no. (FR + RF) of DNA motifs	No. of FR DNA motifs	No. of RF DNA motifs
B2T1	395	262	205
B2T2	398	264	204
B3T1	394	263	203
DNA motifs found in common among replications			
B2T1 and B2T2	394	262	202
B2T1 and B3T1	391	261	202
B2T2 and B3T1	392	262	200
B2T1, B2T2 and B3T1	390	261	199

804

Forward-reverse (FR)

TF	Score 1	Score 2
AHR	38.81	13.41
ARNTL	155.78	1.96
ATF1	323.31	15.00
ATF3	323.31	35.22
BCL	153.72	3.52
CREB	90.91	2.32
CREB3	323.31	38.74
CREB3L1	323.31	27.96
CTCF	323.31	3.50
CTCFL	174.90	2.09
CXXC1	69.92	3.30
E2	323.31	20.15
E2F	122.12	21.87
E2F1	43.22	2.85
EGR1	79.09	3.79
EGR2	176.69	4.53
EGR3	85.25	34.18
EHF	323.31	8.66
ELF1	203.38	3.86
ELF2	227.62	7.83
ELF5	323.31	8.76
ELK1:TBX21	126.46	8.41
ELK1:TEF	323.31	7.99
ELK4	117.83	4.81
ENO1	80.42	3.13
EPAS1	65.43	7.76
ERF	207.67	6.25
ERG	199.81	25.70
ETS	196.80	1.63
ETS1	308.00	3.92

TF	Score 1	Score 2
ETS2	208.78	13.99
ETV1	153.32	7.02
ETV3	140.11	14.58
ETV5:EVX1	145.48	17.33
ETV5:HES7	8.76	8.74
ETV5:TCF3	203.52	5.90
FOXN4	73.43	5.59
FOXO1:ELK3	323.31	43.51
GABPA	197.57	20.39
GABPA:GABPB1	142.28	6.10
GCM2	13.68	18.80
GDNF	286.73	3.15
GMEB1	136.68	10.56
HIC1	223.55	4.56
HIF1A	241.47	1.71
HOXB2:ETV1	102.22	2.42
ID2	323.31	14.52
INSM1	193.85	15.87
JUN:JUNB	275.78	6.48
JUNB:JUN	202.73	5.07
KLF	252.10	8.35
KLF15	323.31	22.56
KLF17	87.51	14.77
KLF2	90.74	15.34
KLF4	209.71	9.38
KLF7	229.95	11.96
LHX8	244.38	2.95
MAX	323.31	8.35
MAZ	109.42	3.37
MBD2	8.41	1.95

TF	Score 1	Score 2
MNT	215.63	8.00
MTF1	323.31	14.21
MXI1	323.31	70.98
MYC	84.79	24.93
MYCN	165.16	25.87
MZF1	81.83	2.29
NFKB1	279.24	14.27
NFKB1:NFKB1	323.31	13.79
NFY	323.31	3.42
NONO	323.31	9.24
NR2C2	323.31	3.64
NRF1	45.13	30.75
OVOL2	323.31	31.61
PATZ1	101.85	9.30
PLAG1	177.90	11.02
PURA	196.04	17.98
R	22.49	3.99
RAD21	258.21	4.81
RBAK	267.43	11.25
RELA	323.31	4.68
RFX1	159.78	17.05
RFX4	323.31	35.28
RFX5	323.31	26.52
SAP1	124.23	14.63
SMC3	222.09	1.76
SP1	235.48	29.09
SP2	94.11	9.54
SP4	14.30	6.31
SPDEF	179.39	16.81
SPIC	323.31	28.49

TF	Score 1	Score 2
STAT	84.60	1.69
STAT1	323.31	5.38
TCF12	111.44	16.79
TCF3	323.31	14.05
TEAD4:ETV4	226.28	5.90
TFAP2A	25.86	20.26
TFAP2B	90.03	6.10
TFAP2C	169.60	8.55
TFAP4	93.98	2.36
TFE3	139.21	16.71
TP73	198.45	7.75
TR4	39.01	4.97
USF1	194.06	3.56
VEZF1	134.36	3.49
XBP1	323.31	44.58
XRCC5:XRCC6	132.56	3.92
YY1	62.59	5.30
ZBED6	183.14	20.23
ZBTB17	48.37	7.27
ZBTB26	151.91	16.84
ZBTB5	120.19	9.58
ZBTB7A	52.89	30.58
ZFX	13.33	14.55
ZFY	36.57	4.04
ZIC3	266.75	10.54
ZIC4	17.27	9.30
ZNF140	323.31	4.99
ZNF143	323.31	35.38
ZNF165	323.31	7.80
ZNF25	281.69	7.72

TF	Score 1	Score 2
ZNF322	120.49	11.55
ZNF325	69.42	2.74
ZNF408	214.73	2.22
ZNF467	127.21	4.64
ZNF479	226.76	3.26
ZNF48	106.17	9.88
ZNF511	84.74	9.87
ZNF553	93.45	9.17
ZNF555	232.83	7.63
ZNF624	235.50	3.84
ZNF672	266.64	10.80
ZNF675	323.31	5.81
ZNF676	323.31	16.54

809

810 Reverse-forward (RF)

TF	Score 1	Score 2	TF	Score 1	Score 2	TF	Score 1	Score 2
ARNT	323.31	14.12	MAX	304.34	8.64	TFE3	95.23	10.59
ARNT2	41.41	42.78	MLXIPL	64.44	10.74	THAP1	127.72	5.07
ASCL2	138.15	6.41	MUSCLE	23.05	3.47	**YY1**	323.31	9.92
ATF3	323.31	14.64	MYB	323.31	17.68	YY2	47.49	2.61
ATF4	323.31	25.14	MYBL1	316.23	23.27	ZBTB33	90.29	7.78
ATF7	79.30	4.96	MYC	323.31	12.23	ZBTB45	323.31	57.08
BCLAF1	148.24	8.52	MZF1	200.49	22.73	ZBTB7A	89.19	16.19
BHLHE40	323.31	12.42	NFY	209.97	3.22	ZBTB7B	43.90	23.59
CDCA7L	84.72	8.42	NFYA	323.31	11.75	ZFP64	147.00	13.59
CREB3	206.55	11.07	NHLH1	105.19	4.42	ZIC3	42.65	15.39
CREB3L1	323.31	7.63	NR1H3	323.31	9.38	ZNF100	27.67	4.75
CREB3L2	67.51	7.98	NR3C1	43.16	8.31	**ZNF143**	63.03	9.69
CTCF	240.61	4.56	OSR2	111.77	14.65	ZNF148	213.77	18.93
E2F	78.16	7.07	RFX1	323.31	22.99	ZNF16	323.31	47.43
E2F1	124.10	15.73	RXRA	146.30	15.11	ZNF37A	310.67	14.79
E2F3	65.67	8.85	SALL1	277.84	1.91	ZNF410	140.45	13.57
E2F6	165.75	30.69	SCRT2	301.48	9.60	ZNF419	247.63	11.25
EFNA2	255.01	10.95	SMAD6	259.24	7.43	ZNF429	87.05	32.39
ELK3	143.48	7.57	SP100	20.75	7.99	ZNF436	323.31	11.48
EP300	121.01	10.90	SP2	294.86	2.59	ZNF468	21.12	7.67
ETV5:CLOCK	42.10	7.29	SP4	110.94	19.63	ZNF557	299.44	9.58
GLIS2	37.40	17.34	SPDEF	185.85	14.35	ZNF575	39.45	14.38
GMEB2	323.31	7.81	SPZ1	323.31	9.87	ZNF586	260.73	6.18
HES1	88.18	9.46	SREBF1	67.27	15.74	ZNF611	279.80	15.65
HES7	166.52	14.60	SREBF2	297.27	1.62	ZNF616	189.53	30.98
HIVEP1	323.31	4.90	TAF1	252.27	17.47	ZNF692	202.47	2.33
HOXB2:ELK1	217.94	11.92	TATA	2.16	4.02	ZNF727	214.01	17.22
IRC900814	323.31	4.89	TFAP2A	20.17	29.15	ZNF770	300.52	4.71
KLF4	213.35	9.49	TFAP2B	29.46	12.62	ZNF773	150.45	8.84
KLF8	323.31	17.42	TFAP2C	112.10	51.21	ZSCAN21	323.31	5.55

811

Forward-reverse (FR)

TF	Score 1	Score 2
AHR	38.81	13.41
ARNTL	155.78	1.96
ATF3	323.31	35.22
BCL	153.72	3.52
CREB3L1	323.31	27.96
CTCF	323.31	3.50
CXXC1	69.92	3.30
E2F	122.12	21.87
E2F1	43.22	2.85
EGR1	79.09	3.79
EGR3	85.25	34.18
ELF1	203.38	3.86
ELF2	227.62	7.83
ELK4	117.83	4.81
ERG	199.81	25.70
ETS	196.80	1.63
ETS1	308.00	3.92
HIC1	223.55	4.56
INSM1	193.85	15.87
KLF4	209.71	9.38
KLF7	229.95	11.96
MAX	323.31	8.35
MYC	84.79	24.93
MYCN	165.16	25.87
MZF1	81.83	2.29
NFY	323.31	3.42
NONO	323.31	9.24
NRF1	45.13	30.75
OVOL2	323.31	31.61
PLAG1	177.90	11.02

TF	Score 1	Score 2
RAD21	258.21	4.81
RFX1	159.78	17.05
SMC3	222.09	1.76
SP2	94.11	9.54
TFAP2A	25.86	20.26
TFAP2B	90.03	6.10
TFAP2C	169.60	8.55
TP73	198.45	7.75
USF1	194.06	3.56
XBP1	323.31	44.58
YY1	62.59	5.30
ZBTB7A	52.89	30.58
ZFX	13.33	14.55
ZNF143	323.31	35.38

Reverse-forward (RF)

TF	Score 1	Score 2
ARNT	323.31	14.12
ATF3	323.31	14.64
BHLHE40	323.31	12.42
CTCF	240.61	4.56
E2F	78.16	7.07
E2F3	65.67	8.85
EFNA2	255.01	10.95
GMEB2	323.31	7.81
KLF4	213.35	9.49
MYB	323.31	17.68
MYC	323.31	12.23
MZF1	200.49	22.73
NFYA	323.31	11.75
NR3C1	43.16	8.31
OSR2	111.77	14.65
SP2	294.86	2.59
SP4	110.94	19.63
SPDEF	185.85	14.35
SREBF2	297.27	1.62
TATA	2.16	4.02
TFAP2B	29.46	12.62
TFAP2C	112.10	51.21
YY1	323.31	9.92
YY2	47.49	2.61
ZBTB33	90.29	7.78
ZBTB7B	43.90	23.59
ZNF100	27.67	4.75
ZNF143	63.03	9.69

Table 3. Correlation of expression level of gene pairs separated by DNA motif sites of a TF. Pairs of genes separated by 64 FR and 52 RF orientations of DNA motif sites of TFs found in common in monocytes, T cells, HMEC and NPC were analyzed to find significantly lower correlation of their expression level than the correlation of all pairs of nearby genes among 53 tissues. Score: $-\log_{10}$ (p-value) of Mann-Whitney test. Median correlation: median correlation coefficient of expression level of nearby gene pairs separated by DNA motif sites. The median correlation coefficient of expression level of all pairs of nearby genes is 0.17. # DNA site: number of DNA motif sites of a TF separating gene pairs with expression data. Ubiquitously expressed genes with

826 coefficient of variance <90 and DNA motif sites nearby were not used for statistical test,
827 so the number of DNA motif sites was relatively small. The results using all genes were
828 shown in Supplemental material. All DNA motif sites of a TF were used including DNA
829 motif sites examined for the biased orientations of DNA motif sites of a TF in EPAs.
830 The results using only the biased orientations of DNA motif sites of a TF were shown in
831 Supplemental material.

832

833 Forward-reverse (FR)

TF	Score	Median correlation	# DNA site
AHR	1.80	0.12	520
ARNT	1.35	0.09	141
ATF2	1.40	0.11	166
ATF3	3.61	0.11	795
BHLHE41	2.02	0.07	118
CREB3L1	2.88	0.05	127
CTCF	6.02	0.09	837
E2F	3.73	0.10	444
E2F1	3.79	0.11	868
EGR1	2.97	0.10	391
ELF1	4.86	0.10	714
ELF2	3.88	0.11	781
ELK3	1.86	0.12	547
ELK4	2.44	0.11	663
ETS	3.34	0.11	523
ETS1	4.27	0.11	687
ETV7	3.68	0.11	662
HIC1	1.65	0.11	380
HINFP	1.33	0.09	258
KLF4	2.00	0.13	718
MYC	3.86	0.11	762
MYCN	2.36	0.11	583
MZF1	1.74	0.10	261
NFYB	2.97	0.10	264
NRF1	2.21	0.11	640
PLAG1	2.93	0.10	503
PLAGL1	2.55	0.10	414
RAD21	6.08	0.09	852
REST	4.35	0.11	920
RFX1	2.38	0.08	81
SIN3A	3.31	0.11	813
SMC3	6.18	0.09	625
SP2	2.30	0.12	738
TFAP2A	4.17	0.11	767
TFAP2C	2.13	0.11	470
USF1	4.24	0.10	628
XBP1	6.65	0.07	379
ZBTB33	4.90	0.10	701
ZBTB7A	2.82	0.10	485
ZFP62	2.95	0.11	565
ZFX	2.69	0.11	581
ZIC1	4.47	0.11	829
ZNF770	3.38	0.08	271

Reverse-forward (RF)

TF	Score	Median correlation	# DNA site
AP1	3.87	0.11	744
ARNT	2.95	0.10	453
ATF3	4.34	0.10	665
BHLHE40	2.49	0.07	155
CREB1	1.79	0.11	303
CTCF	5.96	0.09	721
E2F	3.95	0.10	663
E2F3	4.05	0.09	616
EFNA2	3.51	0.10	543
EGR1	2.58	0.10	428
EGR2	1.39	0.13	747
ETS1	3.75	0.11	667
FLI1:FIGLA	5.41	0.08	428
FOS	3.51	0.11	777
GMEB2	1.36	0.09	310
HIF1A	2.34	0.11	448
KLF4	2.21	0.12	744
MITF	3.14	0.10	419
MYC	4.85	0.10	704
MYCN	2.79	0.10	507
NFKB1	1.59	0.11	342
NFYA	2.15	0.10	229
NRF1	2.01	0.12	615
OSR2	1.99	0.12	301
PBX3	2.20	0.11	253
RFX2	2.12	0.09	168
RFX5	3.03	0.05	75
RUNX3	2.01	0.11	241
SP1	2.73	0.11	725
SP2	2.15	0.12	1090
SP4	2.33	0.11	479
SPDEF	5.29	0.07	449
TFAP2B	3.42	0.11	855
TFAP2C	2.05	0.11	576
TFCP2L1	1.45	0.13	362
YBX1	1.34	0.13	160
YY1	2.23	0.01	50
ZBTB33	3.44	0.11	886
ZBTB7B	2.27	0.13	892
ZNF143	2.26	0.07	81

834

835 **Table 4.** Top 30 of co-location and overlapping biased orientations of DNA binding
836 motif sequences of TFs in monocytes. Co-location and overlapping DNA motif
837 sequences of CTCF with another biased orientation of DNA motif sequence were shown
838 in separate tables. Motif 1,2: DNA binding motif sequences of TFs. No.: the number of
839 genomic locations with both Motif 1 and Motif 2 in upstream and downstream of genes
840 in EPAs (< 1 Mb distance from TSS of genes). Total number of genes is 30,523.

841

842 Forward-reverse (FR)

Motif 1	Motif 2	No.	Mean of distances bet. DNA sites (nt)	Median of distances bet. DNA sites (nt)	Mean of distances from TSS (nt)	Median of distances from TSS (nt)	Interquartile range of distance from TSS (nt)
FOS	JUN	3332	0.00	0	43202.95	18085	5524 - 48583
CTCF	**SMC3**	2876	0.01	0	34606.92	13716	3073 - 39471
FOSL2	JUN	2807	0.00	0	40389.84	17365	5424 - 45251
FOSB	FOSL2	2644	0.00	0	44302.93	17867	5633 - 47209
EGR1	EGR2	2397	0.00	0	14578.21	1251	247 - 11473
CTCF	**RAD21**	2352	0.00	0	33492.68	12913	2824 - 37672
RAD21	**SMC3**	2343	0.02	0	33572.80	14302	3856 - 37159
ATF3	FOSL2	2322	0.00	0	42784.04	17841	5366 - 48236
FOSL2	JUNB	2305	0.02	0	42884.36	17867	5706 - 46515
ETS2	ETSLIKE	2205	0.00	0	37660.66	15765	4146 - 41462
FOS	JUNB	2151	0.00	0	38403.20	16367	4849 - 44736
IRF	IRF4	1962	0.00	0	40794.41	15872	3969 - 45946
FOSL2	SMARCC1	1945	0.00	0	42429.69	17369	5094 - 46586
EGR1	WT1	1941	0.16	0	12485.23	427	93 - 5394
FOSB	JUN	1808	0.02	0	36648.74	16705	5156 - 40309
ATF3	JUN	1713	0.02	0	38101.24	17119	5294 - 43559
JUN	TFAP2A	1628	0.00	0	42262.97	18017	5089 - 47094
FOSL2	TFAP2A	1628	0.00	0	36606.38	16201	4949 - 41948
BACH2	SMARCC1	1462	0.16	0	38673.02	14778	4060 - 41262
ELF1	ETS1	1459	0.00	0	37056.72	14346	3370 - 40339
CHD2	E2F	1429	0.00	0	19220.38	1579	329 - 16257
JUN	NR3C1	1262	0.00	0	35052.17	14418	3844 - 38534
USF1	USF2	1260	0.00	0	25188.91	4726	413 - 24699
BACH2	JUNB	1238	0.15	0	36252.37	15302	4462 - 39393
BACH2	FOSB	1184	0.22	0	37190.80	14778	4038 - 41262
ETSLIKE	GABPA	1164	0.00	0	32352.24	11683	2356 - 36919
CTCF	CTCFL	1151	0.00	0	30252.04	11606	2229 - 34539
NR5A1	NR5A2	1133	0.00	0	41171.86	12243	2488 - 43136
ATF3	BACH2	1094	0.18	0	35659.16	13605	3821 - 39756
ETS2	GABPA	1092	0.06	0	27250.24	12184	2858 - 32196

843

844

845

846

Reverse-forward (RF)

Motif 1	Motif 2	No.	Mean of distances bet. DNA sites (nt)	Median of distances bet. DNA sites (nt)	Mean of distances from TSS (nt)	Median of distances from TSS (nt)	Interquartile range of distance from TSS (nt)
EGR1	EGR3	3012	0.00	0	17005.00	709	149 - 10393
NR1I2	NR1I3	2932	0.00	0	49622.84	20548	5924 - 58436
ZIC1	ZIC3	2871	0.07	0	21511.64	3092	434 - 19128
EGR	WT1	2612	0.04	0	9949.38	396	102 - 4266
FOS	FOS:JUN	2512	0.01	0	37200.80	15466	4438 - 42373
EGR	EGR3	2293	0.17	0	11634.92	532	135 - 6044
MAFG	NFE2L1:MAFG	2272	0.03	0	34641.56	16917	5284 - 42097
KLF10	SP1	2233	0.00	0	9778.94	297	73 - 3077
EGR	EGR2	2160	0.16	0	10502.76	490	129 - 5227
KLF3	SP3	2036	0.00	0	6974.78	246	63 - 1447
KLF1	SP3	1771	0.00	0	7748.42	264	66 - 1829
KLF10	SP3	1734	0.00	0	7275.48	222	58 - 1320
KLF7	SP4	1639	0.00	0	12521.62	309	58 - 4894
KLF1	SP1	1574	0.05	0	6780.46	245	61 - 1438
AP1	JUNB	1572	0.05	0	34158.07	15451	4746 - 40315
EGR1	WT1	1543	0.31	0	12742.28	444	111 - 5553
EGR1	SP1:SP3	1393	0.08	0	7789.54	307	91 - 1886
FOS:JUN	JUNB	1386	0.14	0	33012.80	14245	3900 - 37988
SP1	SP3	1372	0.00	0	8845.31	293	77 - 1816
EHF	ELF1	1366	0.02	0	41217.39	13357	2842 - 43178
CTCF	RXRA	1362	0.00	0	29981.33	10937	2100 - 31407
AP1	FOS	1327	0.03	0	33225.52	13455	3503 - 37399
ATF1	ATF3	1215	0.00	0	23125.06	3798	342 - 21091
ELK1	ZNF200	1156	0.05	0	22200.49	2883	181 - 17610
SP1	SP4	1137	0.00	0	7371.85	215	63 - 1232
EHF	ELF3	1134	0.00	0	36296.46	10912	596 - 37318
MEIS2	TGIF1	1018	0.00	0	47677.15	17654	3273 - 49233
KLF3	SP1	1017	0.06	0	6514.33	226	60 - 994
SPI1	ZNF200	913	0.06	0	10962.81	425	85 - 6046
AP1	FOS:JUN	860	0.09	0	50412.92	24217	7302 - 60018

FR orientation of CTCF

Motif 1	Motif 2	No.	Mean of distances bet. DNA sites (nt)	Median of distances bet. DNA sites (nt)	Mean of distances from TSS (nt)	Median of distances from TSS (nt)	Interquartile range of distance from TSS (nt)
CTCF	SMC3	2876	0.01	0	34606.92	13716	3073 - 39471
CTCF	RAD21	2352	0.00	0	33492.68	12913	2824 - 37672
CTCF	CTCFL	1151	0.00	0	30252.04	11606	2229 - 34539
CTCF	ZBTB7A	470	0.27	0	23227.96	7065	745 - 23496
CTCF	E2F	123	0.81	0	7913.36	222	61 - 1997
CTCF	WT1	120	0.00	0	3543.72	114	44 - 375
CTCF	MYC	110	2.30	0	31289.45	11948	2887 - 33972

RF orientation of CTCF

Motif 1	Motif 2	No.	Mean of distances bet. DNA sites (nt)	Median of distances bet. DNA sites (nt)	Mean of distances from TSS (nt)	Median of distances from TSS (nt)	Interquartile range of distance from TSS (nt)
CTCF	RXRA	1362	0.00	0	29981.33	10937	2100 - 31407
CTCF	CTCFL	429	0.00	0	25171.22	9834	1859 - 24741
CTCF	RAD21	337	0.00	0	38829.91	17973	6117 - 45749
CTCF	ZIC1	126	1.40	0	35480.65	10286	2316 - 29380
CTCF	ZIC3	108	0.00	0	30219.32	10904	4463 - 31037

References

Ackerman SL, Minden AG, Williams GT, Bobonis C, Yeung CY. 1991. Functional significance of an overlapping consensus binding motif for Sp1 and Zif268 in the murine adenosine deaminase gene promoter. *Proc Natl Acad Sci U S A* **88**: 7523-7527.

Ansari AZ, Peterson-Kaufman KJ. 2011. A partner evokes latent differences between Hox proteins. *Cell* **147**: 1220-1221.

Bailey SD, Zhang X, Desai K, Aid M, Corradin O, Cowper-Sal Lari R, Akhtar-Zaidi B, Scacheri PC, Haibe-Kains B, Lupien M. 2015. ZNF143 provides sequence specificity to secure chromatin interactions at gene promoters. *Nat Commun* **2**: 6186.

Barutcu AR, Lajoie BR, Fritz AJ, McCord RP, Nickerson JA, van Wijnen AJ, Lian JB, Stein JL, Dekker J, Stein GS et al. 2016. SMARCA4 regulates gene expression and higher-order chromatin structure in proliferating mammary epithelial cells. *Genome research* **26**: 1188-1201.

Chatterjee R, Zhao J, He X, Shlyakhtenko A, Mann I, Waterfall JJ, Meltzer P, Sathyanarayana BK, FitzGerald PC, Vinson C. 2012. Overlapping ETS and CRE Motifs ((G/C)CGGAAGTGACGTCA) preferentially bound by GABPalpha and CREB proteins. *G3 (Bethesda)* **2**: 1243-1256.

Chen M, Manley JL. 2009. Mechanisms of alternative splicing regulation: insights from molecular and genomics approaches. *Nat Rev Mol Cell Biol* **10**: 741-754.

Das D, Clark TA, Schweitzer A, Yamamoto M, Marr H, Arribere J, Minovitsky S, Poliakov A, Dubchak I, Blume JE et al. 2007. A correlation with exon expression approach to identify cis-regulatory elements for tissue-specific alternative splicing. *Nucleic acids research* **35**: 4845-4857.

de Wit E, Vos ES, Holwerda SJ, Valdes-Quezada C, Verstegen MJ, Teunissen H, Splinter E, Wijchers PJ, Krijger PH, de Laat W. 2015. CTCF Binding Polarity Determines Chromatin Looping. *Molecular cell* **60**: 676-684.

Guo Y, Xu Q, Canzio D, Shou J, Li J, Gorkin DU, Jung I, Wu H, Zhai Y, Tang Y et al. 2015. CRISPR Inversion of CTCF Sites Alters Genome Topology and Enhancer/Promoter Function. *Cell* **162**: 900-910.

He X, Syed KS, Tillo D, Mann I, Weirauch MT, Vinson C. 2015. GABPalpha Binding to Overlapping ETS and CRE DNA Motifs Is Enhanced by CREB1: Custom DNA Microarrays. *G3 (Bethesda)* **5**: 1909-1918.

Hsu SC, Gilgenast TG, Bartman CR, Edwards CR, Stonestrom AJ, Huang P, Emerson DJ, Evans P, Werner MT, Keller CA et al. 2017. The BET Protein BRD2 Cooperates with CTCF to Enforce Transcriptional and Architectural Boundaries. *Molecular cell* **66**: 102-116 e107.

Ji X, Dadon DB, Abraham BJ, Lee TI, Jaenisch R, Bradner JE, Young RA. 2015. Chromatin proteomic profiling reveals novel proteins associated with histone-marked genomic regions. *Proc Natl Acad Sci U S A* **112**: 3841-3846.

Jolma A, Yan J, Whitington T, Toivonen J, Nitta KR, Rastas P, Morgunova E, Enge M, Taipale M, Wei G et al. 2013. DNA-binding specificities of human transcription factors. *Cell* **152**: 327-339.

Jolma A, Yin Y, Nitta KR, Dave K, Popov A, Taipale M, Enge M, Kivioja T, Morgunova E, Taipale J. 2015. DNA-dependent formation of transcription factor pairs alters their binding specificity. *Nature* **527**: 384-388.

Jung I, Schmitt A, Diao Y, Lee AJ, Liu T, Yang D, Tan C, Eom J, Chan M, Chee S et al. 2019. A compendium of promoter-centered long-range chromatin interactions in the human genome. *Nature genetics* **51**: 1442-1449.

Karolchik D, Barber GP, Casper J, Clawson H, Cline MS, Diekhans M, Dreszer TR, Fujita PA, Guruvadoo L, Haeussler M et al. 2014. The UCSC Genome Browser database: 2014 update. *Nucleic acids research* **42**: D764-770.

Katainen R, Dave K, Pitkanen E, Palin K, Kivioja T, Valimaki N, Gylfe AE, Ristolainen H, Hanninen UA, Cajuso T et al. 2015. CTCF/cohesin-binding sites are frequently mutated in cancer. *Nature genetics* **47**: 818-821.

Kel AE, Gossling E, Reuter I, Cheremushkin E, Kel-Margoulis OV, Wingender E. 2003. MATCH: A tool for searching transcription factor binding sites in DNA sequences. *Nucleic acids research* **31**: 3576-3579.

Kheradpour P, Kellis M. 2014. Systematic discovery and characterization of regulatory motifs in ENCODE TF binding experiments. *Nucleic acids research* **42**: 2976-2987.

Kin K, Chen X, Gonzalez-Garay M, Fakhouri WD. 2016. The effect of non-coding DNA variations on P53 and cMYC competitive inhibition at cis-overlapping

motifs. *Hum Mol Genet* **25**: 1517-1527.

Kulakovskiy IV, Vorontsov IE, Yevshin IS, Sharipov RN, Fedorova AD, Rumynskiy EI, Medvedeva YA, Magana-Mora A, Bajic VB, Papatsenko DA et al. 2018. HOCOMOCO: towards a complete collection of transcription factor binding models for human and mouse via large-scale ChIP-Seq analysis. *Nucleic acids research* **46**: D252-D259.

Li H, Durbin R. 2009. Fast and accurate short read alignment with Burrows-Wheeler transform. *Bioinformatics (Oxford, England)* **25**: 1754-1760.

Lieberman-Aiden E, van Berkum NL, Williams L, Imakaev M, Ragoczy T, Telling A, Amit I, Lajoie BR, Sabo PJ, Dorschner MO et al. 2009. Comprehensive mapping of long-range interactions reveals folding principles of the human genome. *Science (New York, NY)* **326**: 289-293.

McLean CY, Bristor D, Hiller M, Clarke SL, Schaar BT, Lowe CB, Wenger AM, Bejerano G. 2010. GREAT improves functional interpretation of cis-regulatory regions. *Nature biotechnology* **28**: 495-501.

Merabet S, Mann RS. 2016. To Be Specific or Not: The Critical Relationship Between Hox And TALE Proteins. *Trends Genet* **32**: 334-347.

Mumbach MR, Satpathy AT, Boyle EA, Dai C, Gowen BG, Cho SW, Nguyen ML, Rubin AJ, Granja JM, Kazane KR et al. 2017. Enhancer connectome in primary human cells identifies target genes of disease-associated DNA elements. *Nature genetics* **49**: 1602-1612.

Neph S, Kuehn MS, Reynolds AP, Haugen E, Thurman RE, Johnson AK, Rynes E, Maurano MT, Vierstra J, Thomas S et al. 2012. BEDOPS: high-performance genomic feature operations. *Bioinformatics (Oxford, England)* **28**: 1919-1920.

Newburger DE, Bulyk ML. 2009. UniPROBE: an online database of protein binding microarray data on protein-DNA interactions. *Nucleic acids research* **37**: D77-82.

Osato N. 2018. Characteristics of functional enrichment and gene expression level of human putative transcriptional target genes. *BMC Genomics* **19**: 957.

Phanstiel DH, Van Bortle K, Spacek D, Hess GT, Shamim MS, Machol I, Love MI, Aiden EL, Bassik MC, Snyder MP. 2017. Static and Dynamic DNA Loops form AP-1-Bound Activation Hubs during Macrophage Development. *Molecular cell* **67**: 1037-1048.e1036.

954 Portales-Casamar E, Thongjuea S, Kwon AT, Arenillas D, Zhao X, Valen E, Yusuf D,
955 Lenhard B, Wasserman WW, Sandelin A. 2010. JASPAR 2010: the greatly
956 expanded open-access database of transcription factor binding profiles. *Nucleic*
957 *acids research* **38**: D105-110.
958 Purmann A, Toedling J, Schueler M, Carninci P, Lehrach H, Hayashizaki Y, Huber W,
959 Sperling S. 2007. Genomic organization of transcriptomes in mammals:
960 Coregulation and cofunctionality. *Genomics* **89**: 580-587.
961 Rao SS, Huntley MH, Durand NC, Stamenova EK, Bochkov ID, Robinson JT, Sanborn
962 AL, Machol I, Omer AD, Lander ES et al. 2014. A 3D map of the human
963 genome at kilobase resolution reveals principles of chromatin looping. *Cell* **159**:
964 1665-1680.
965 Schreiber J, Libbrecht M, Bilmes J, Noble W. 2017. Nucleotide sequence and DNaseI
966 sensitivity are predictive of 3D chromatin architecture. *bioRxiv*.
967 Sherwood RI, Hashimoto T, O'Donnell CW, Lewis S, Barkal AA, van Hoff JP, Karun V,
968 Jaakkola T, Gifford DK. 2014. Discovery of directional and nondirectional
969 pioneer transcription factors by modeling DNase profile magnitude and shape.
970 *Nature biotechnology* **32**: 171-178.
971 Shlyueva D, Stampfel G, Stark A. 2014. Transcriptional enhancers: from properties to
972 genome-wide predictions. *Nature reviews Genetics* **15**: 272-286.
973 Shrivastava A, Calame K. 1994. An analysis of genes regulated by the multi-functional
974 transcriptional regulator Yin Yang-1. *Nucleic acids research* **22**: 5151-5155.
975 Slattery M, Riley T, Liu P, Abe N, Gomez-Alcala P, Dror I, Zhou T, Rohs R, Honig B,
976 Bussemaker HJ et al. 2011. Cofactor binding evokes latent differences in DNA
977 binding specificity between Hox proteins. *Cell* **147**: 1270-1282.
978 Tabuchi TM, Deplancke B, Osato N, Zhu LJ, Barrasa MI, Harrison MM, Horvitz HR,
979 Walhout AJ, Hagstrom KA. 2011. Chromosome-biased binding and gene
980 regulation by the Caenorhabditis elegans DRM complex. *PLoS Genet* **7**:
981 e1002074.
982 van Helden J. 2003. Regulatory sequence analysis tools. *Nucleic acids research* **31**:
983 3593-3596.
984 Wang ET, Sandberg R, Luo S, Khrebtukova I, Zhang L, Mayr C, Kingsmore SF,
985 Schroth GP, Burge CB. 2008. Alternative isoform regulation in human tissue
986 transcriptomes. *Nature* **456**: 470-476.

987 Wang J, Zhuang J, Iyer S, Lin X, Whitfield TW, Greven MC, Pierce BG, Dong X,
988 Kundaje A, Cheng Y et al. 2012a. Sequence features and chromatin structure
989 around the genomic regions bound by 119 human transcription factors. *Genome*
990 *research* **22**: 1798-1812.
991 Wang L, Wang S, Li W. 2012b. RSeQC: quality control of RNA-seq experiments.
992 *Bioinformatics (Oxford, England)* **28**: 2184-2185.
993 Wei Z, Gao F, Kim S, Yang H, Lyu J, An W, Wang K, Lu W. 2013. Klf4 organizes
994 long-range chromosomal interactions with the oct4 locus in reprogramming and
995 pluripotency. *Cell Stem Cell* **13**: 36-47.
996 Weintraub AS, Li CH, Zamudio AV, Sigova AA, Hannett NM, Day DS, Abraham BJ,
997 Cohen MA, Nabet B, Buckley DL et al. 2017. YY1 Is a Structural Regulator of
998 Enhancer-Promoter Loops. *Cell* **171**: 1573-1588 e1528.
999 Wingender E, Dietze P, Karas H, Knuppel R. 1996. TRANSFAC: a database on
1000 transcription factors and their DNA binding sites. *Nucleic acids research* **24**:
1001 238-241.
1002 Xi H, Yu Y, Fu Y, Foley J, Halees A, Weng Z. 2007. Analysis of overrepresented motifs
1003 in human core promoters reveals dual regulatory roles of YY1. *Genome research*
1004 **17**: 798-806.
1005 Xie X, Mikkelsen TS, Gnirke A, Lindblad-Toh K, Kellis M, Lander ES. 2007.
1006 Systematic discovery of regulatory motifs in conserved regions of the human
1007 genome, including thousands of CTCF insulator sites. *Proc Natl Acad Sci U S A*
1008 **104**: 7145-7150.
1009 Xie Z, Hu S, Blackshaw S, Zhu H, Qian J. 2010. hPDI: a database of experimental
1010 human protein-DNA interactions. *Bioinformatics (Oxford, England)* **26**:
1011 287-289.
1012 Yardimci GG, Ozadam H, Sauria MEG, Ursu O, Yan KK, Yang T, Chakraborty A, Kaul
1013 A, Lajoie BR, Song F et al. 2019. Measuring the reproducibility and quality of
1014 Hi-C data. *Genome Biol* **20**: 57.
1015 Yoon SO, Chikaraishi DM. 1992. Tissue-specific transcription of the rat tyrosine
1016 hydroxylase gene requires synergy between an AP-1 motif and an overlapping E
1017 box-containing dyad. *Neuron* **9**: 55-67.
1018 Zhang H, Li F, Jia Y, Xu B, Zhang Y, Li X, Zhang Z. 2017. Characteristic arrangement
1019 of nucleosomes is predictive of chromatin interactions at kilobase resolution.

Nucleic acids research **45**: 12739-12751.

Zhang Y, Liu T, Meyer CA, Eeckhoute J, Johnson DS, Bernstein BE, Nusbaum C, Myers RM, Brown M, Li W et al. 2008. Model-based analysis of ChIP-Seq (MACS). *Genome Biol* **9**: R137.

Zhao Y, Stormo GD. 2011. Quantitative analysis demonstrates most transcription factors require only simple models of specificity. *Nature biotechnology* **29**: 480-483.